Design and Synthesis of Potent Inhibitors of the Malaria Aspartyl Proteases Plasmepsin I and II. Use of Solid-Phase Synthesis to Explore Novel Statine Motifs

Per-Ola Johansson,[†] Yantao Chen,[†] Anna Karin Belfrage,[†] Michael J. Blackman,[‡] Ingemar Kvarnström,[†] Katarina Jansson,[§] Lotta Vrang,[§] Elizabeth Hamelink,[§] Anders Hallberg,[∥] Åsa Rosenquist,*[,†,§] and Bertil Samuelsson*[,§,⊥]

Department of Chemistry, Linköping University, S-581 83 Linköping, Sweden, Division of Parasitology, National Institute for Medical Research, The Ridgeway, Mill Hill, London NW7 1AA, UK, Medivir AB, Lunastigen 7, S-141 44 Huddinge, Sweden, Department of Medicinal Chemistry, Uppsala University, BMC, Box 574, S-751 23 Uppsala, Sweden, and Department of Organic Chemistry, Arrhenius Laboratory, Stockholm University, S-106 91 Stockholm, Sweden

Received November 19, 2003

Picomolar to low nanomolar inhibitors of the two aspartic proteases plasmepsin (Plm) I and II, from the malaria parasite *Plasmodium falciparum,* have been identified from sets of libraries containing novel statine-like templates modified at the amino and carboxy terminus. The syntheses of the novel statine templates were carried out in solution phase using efficient synthetic routes and resulting in excellent stereochemical control. The most promising statine template was attached to solid support and diversified by use of parallel synthesis. The products were evaluated for their Plm I and II inhibitory activity as well as their selectivity over cathepsin D. Selected inhibitors were, in addition, evaluated for their inhibition of parasite growth in cultured infected human red blood cells. The most potent inhibitor in this report, compound **16**, displays K_i values of 0.5 and 2.2 nM for Plm I and II, respectively. Inhibitor **16** is also effective in attenuating parasite growth in red blood cells showing 51% inhibition at a concentration of 5 μM. Several inhibitors have been identified that exhibit K_i values between 0.5 and 74 nM for both Plm I and II. Some of these inhibitors also show excellent selectivity vs cathepsin D.

Introduction

Malaria is considered as one of the most serious infectious diseases in the world, affecting approximately 500 million people. It is estimated that the annual mortality from malaria is 2 million, and that more than 40% of the world's population is at risk of infection.[1] The disease is spread by the *Anopheles* mosquito, mostly found in the tropical regions of the world, although not all species of the mosquito transmit malaria.[2] There are four major species of the malaria parasite, i.e. *Plasmodium falciparum*, *P. vivax*, *P. malariae*, and *P. ovale*,[1a] of which *P. falciparum* is responsible for more than 95% of malaria-related morbidity and mortality. Increasingly *P. falciparum* is becoming resistant to existing therapies, including e.g. chloroquine, mefloquine, and sulfadoxime/pyrimethamine, and there are strains of *P. falciparum* reported to be resistant to all known antimalarial therapies with potentially devastating consequences in particular for the developing world. This has been recognized as a major health concern, highlighting the urgent need for new treatment paradigms and for new efficacious drugs to combat this disease.[1a,3]

In the erythrocytic stage of the parasite's life cycle the parasite invades the red blood cells of its host consuming up to 80% of the hemoglobin as a source of nutrients for growth and development. Hemoglobin degradation takes place in an acidic food vacuole of the parasite and many of the current antimalarial drugs appear to disrupt important vacuolar functions.[4a] The food vacuole contains aspartic, cysteine, and metallo proteases, which are all considered to play a role in the process of hemoglobin degradation. At least 10 genes encoding aspartic proteases have been identified in the *P. falciparum* genome, potentially complicating the picture of target selection and target redundancy.[5] Four of the aspartic proteases have been localized to the acidic food vacuole of the parasite, namely plasmepsin I, II, IV, and HAP, a histo-aspartic protease.[1e,f,6] The parasite cysteine proteases falcipain 1−3 and the aspartic proteases plasmepsin I and II (Plm I and II) have been studied in detail, and inhibitors of these falcipains and plasmepsins have shown efficacy in cell and animal models of malaria, indicating that these enzymes may be suitable molecular targets for drug discovery.[7]

The two plasmepsins I and II show a high degree of sequence homology (73%), suggesting that both enzymes can be inhibited by similar compounds. However, they also show structural similarity with human cathepsin D, making selectivity an important factor in inhibitor design.[3,8] Several structural motifs have been pursued in the design and synthesis of Plm I and II inhibitors mimicking the tetrahedral intermediate formed during the aspartyl protease catalysis.[3,4,8−10] These motifs include hydroxyethylamines,[3,10a,b] C_2-symmetric dipeptide mimetics,[8,10e,f] and reversed-statines.[10c,d]

* Corresponding authors. Phone: +46 8 54683100. Fax: +46 8 54683199. E-mail: bertil.samuelsson@medivir.se; asa.rosenquist@medivir.se.
[†] Linköping University.
[‡] National Institute for Medical Research.
[§] Medivir AB.
[∥] Uppsala University.
[⊥] Stockholm University.

10.1021/jm031106i CCC: $27.50
Published on Web 05/26/2004

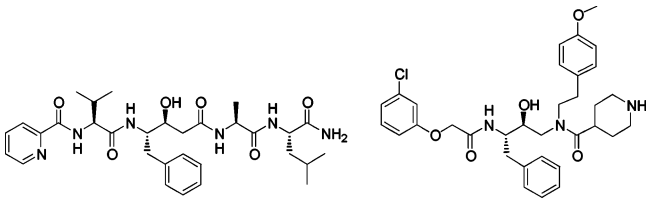

A[4] (K_i Plm I: 16 nM)[4b] (K_i Plm II: 0.56 nM)[4a] (K_i Cat D: 21 nM)[4a]

B[3] (K_i Plm II: 4.3 nM) (K_i Cat D: 63 nM)

Figure 1. Two potent plasmepsin inhibitors encompassing a modified statine (**A**) and a hydroxyethylamine (**B**) motif.

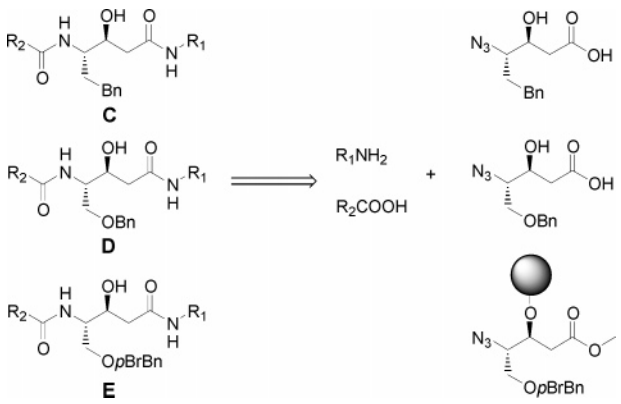

Figure 2. Synthetic approach toward the statine mimetic plasmepsin inhibitors.

The crystal structure of Plm II in complex with pepstatin A has been reported. Pepstatin A is a highly potent peptidic inhibitor of Plm II showing a K_i value of 0.006 nM, suggesting that the statine core may well serve as a useful starting point for the design of new and selective antimalarial compounds.[4a] This strategy has previously been successfully employed resulting in the development of potent plasmepsin I and II inhibitors,[4,9b–d] e.g. inhibitor **A**[4] which shows K_i values of 16 nM and 0.56 nM for Plm I and II, respectively, and show in vivo activity, albeit low, in a parasite growth assay[11] exhibiting 54% inhibition at a concentration of 20 μM (Figure 1). The selectivity for this inhibitor toward cathepsin D is, however, moderate displaying a K_i value of 21 nM against cathepsin D. A potent inhibitor, compound **B**,[3] incorporating the hydroxyethylamine template is also exemplified in Figure 1.

Previous studies have shown that Plm II has a continuous S1−S3 crevice that potentially could accommodate large P1 substituents.[3,4a] We have in this study focused on P1 modifications in the phenyl statine core of inhibitor **A**, i.e. compounds **C**, **D**, and **E** shown in Figure 2, as a useful starting point toward novel and improved inhibitors of plasmepsin I and II. The homologue of compound **A** extending the P1 substituent with one carbon (compound **C,** Figure 2, compound **14**, Scheme 4 and Table 1) was initially prepared and assayed. This inhibitor was less potent against both Plm I and II than the reference inhibitor **A**, displaying K_i values of 27 nM and 46 nM respectively for Plm I and II (Table 1).

Previous work from our laboratories has shown that insertion of an oxygen atom in the appropriate position of a peptidomimetic or dipeptidomimetic structure not only introduces a new useful center for diversification but can lead to simplified synthesis and provide increased potency against desired proteases.[10e,12] With this in mind, the benzyloxy statine inhibitor **15** was synthesized (compound **D**, Figure 2, Scheme 4 and Table 1) which delivered an increase in potency compared to compound **14** with K_i values of 5.4 nM and 11 nM for

Table 1

Compd	Structure	Yield (5 steps)	K_i (nM) Plm I	K_i (nM) Plm II	K_i (nM) Cat D	RBC[b] Inh @ 5 μM
A	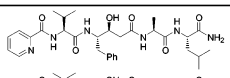	-	16[4b]	0.56[4a]	21[4a]	54 % @ 20 μM[4a]
14	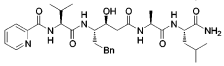	31 %[a]	27	46	980	41 %
15	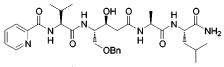	27 %[a]	5.4	11	41	37 %
16	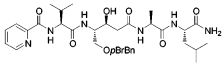	20 %	0.5	2.2	4.9	51 %
17	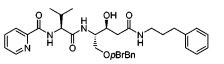	21 %	5.4	30	459	ND
18	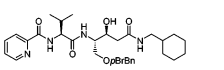	15 %	3.9	41	586	ND
19	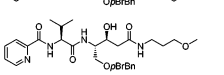	15 %	49	248	>4000	ND
20	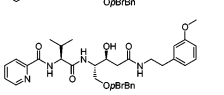	21 %	6.7	29	140	25 %
21	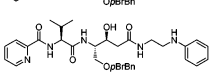	19 %	8.9	74	265	25 %
22	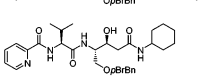	20 %	4.1	25	217	21 %
23	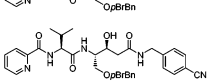	19 %	53	256	623	ND
24	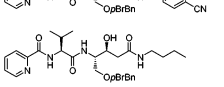	19 %	8.1	68	473	ND
25	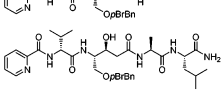	18 %	6.4	15	41	50 %
26	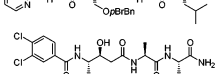	42 %	32	91	1807	ND
27	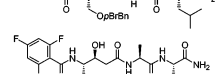	29 %	3.4	10	>4000	10 %
28	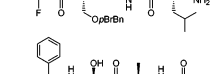	27 %	57	139	52	10 %
29	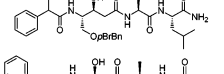	25 %	40	284	100	ND
30	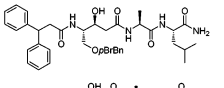	29 %	24	348	35	ND
31	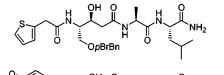	10 %	29	131	>5900	ND
32	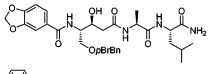	31 %	59	144	322	16 %
33	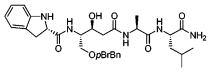	24 %	619	390	>5900	29 %
34	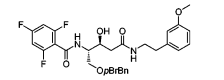	27 %	822	230	>5900	0 %

[a] Synthesized in solution and the yield is over three steps. [b] ND = not determined.

Scheme 1[a]

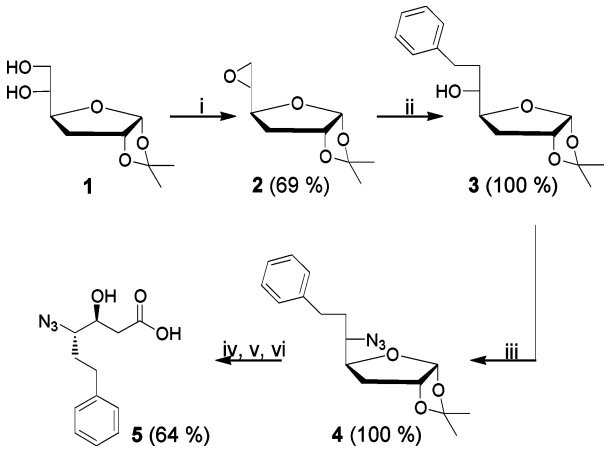

[a] Reagents and conditions: (i) DIAD, PPh_3, $CHCl_3$, reflux; (ii) benzylmagnesium chloride, THF; (iii) PPh_3, DIAD, DPPA, THF; (iv) HOAc/H_2O 1:1, 115 °C; (v) $NaIO_4$, $KMnO_4$; (vi) 1 M NaOH.

Plm I and II, respectively. Further refinement in the aromatic portion of the P1 position resulted in the synthesis of inhibitor **16** having a *p*-bromobenzyloxy P1 statine substituent (compounds **E,** Figure 2, Table 1), which delivered very impressive K_i values of 0.5 nM and 2.2 nM, respectively for Plm I and II and moreover exerted an encouraging inhibition of parasite growth of 51% at 5 μM concentration. The cathepsin D selectivity was however moderate (K_i value of 4.9 nM) but viewed as amenable to further optimization. On the basis of these encouraging results, the *p*-bromobenzyloxy P1 statine template was selected as a model and was diversified in the P and P′ positions. The synthesis of this building block was straightforward starting from D-glucose, as depicted in Scheme 2. The substitutions of the amino and carboxy terminus were carried out on solid support (Figure 2, Scheme 5) furnishing the inhibitors **16**−**34** (Table 1).

The compounds synthesized, **14**−**34**, were evaluated for their Plm I and II inhibitory activity as well as for their selectivity over cathepsin D. Selected compounds were tested for inhibition of parasite growth in culture. The most promising inhibitors identified show K_i values in the 0.5−74 nM range for both Plm I and II, and with 2−1100-fold selectivity over cathepsin D. The best inhibitor, **16**, exhibits 51% inhibition of parasite growth at 5 μM concentration.

Results and Discussion

Chemistry. For the synthesis of compounds **C** (Figure 2) the pivotal intermediate (**5**)[13] was used (Scheme 1). Starting from diacetone D-glucose, 3-deoxy-1,2-*O*-isopropylidene-D-glucose (**1**) was synthesized in an overall yield of 68% over three steps according to literature procedure.[14] Reacting **1** with diisopropyl azodicarboxylate (DIAD) and triphenylphosphine in refluxing chloroform[15] delivered epoxide (**2**)[13,16] in 69% yield. Regioselective opening of the epoxide (**2**) at the sterically least hindered site with benzylmagnesium chloride in dry THF gave compound **3** in ∼100% yield.[13,17] Subsequent treatment of **3** under Mitsunobu-like conditions using triphenylphosphine, DIAD, and diphenylphosphoryl azide (DPPA) in THF provided the corresponding azide (**4**) with inversion of configuration in quantitative

Scheme 2[a]

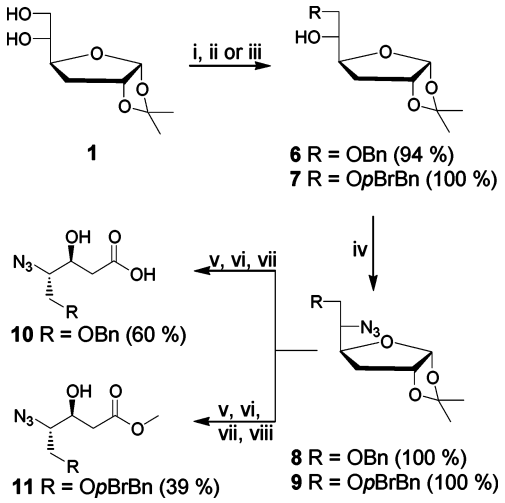

[a] Reagents and conditions: (i) Bu_2SnO, toluene, reflux; (ii) tetrabutylammonium bromide, BnBr, toluene 90 °C; (iii) tetrabutylammonium bromide, *p*BrBnBr, toluene, 90 °C; (iv) PPh_3, DIAD, DPPA, THF; (v) HOAc/H_2O 1:1, 115 °C; (vi) $NaIO_4$, $KMnO_4$; (vii) 1 M NaOH; (viii) AcCl, MeOH.

yield.[18] Initially diethyl azodicarboxylate (DEAD) was employed in this reaction; however, due to problematic purifications and unsatisfying yields the related DIAD was employed which resulted in excellent yield of product **4**. Subsequently the isopropylidene group of **4** was hydrolyzed using 50% aqueous acetic acid at 115 °C affording the corresponding diol which was thereafter oxidized with sodium periodate in the presence of a catalytic amount of potassium permanganate to generate a mixture of carboxylic acid **5** and its corresponding formic ester. Hydrolysis of the mixture using 1 M aqueous sodium hydroxide produced compound **5** in 64% yield over the three steps.[13]

For the synthesis of the two azido benzyloxy scaffolds **10** and **11** (Scheme 2), of the generic structures **D** and **E** (Figure 2), similar synthetic routes as used for the synthesis **5** were employed (Scheme 1). Selective alkylation of the primary hydroxyl group in compound **1** was performed by reacting **1** with dibutyltin oxide in toluene followed by benzyl bromide and tetrabutylammonium bromide furnishing the corresponding 6-*O*-benzylated compound **6** in 94% yield.[19] Compound **7** was obtained in ∼100% yield using the same procedure but employing *p*-bromobenzyl bromide as alkylating agent. Compound **6** and **7** were then transformed to their corresponding azides **8** and **9** (Scheme 2) in quantitative yields. The benzyloxy derivative **10** was obtained in 60% yield over the three steps from **8,** according to the synthesis of **5**. The *p*-bromobenzyloxy scaffold **11** was delivered from **9** also according to the same procedure as used in the synthesis of **5** with the exception that the crude acid product was directly transformed into the corresponding methyl ester by treatment with acidic methanol which yielded **11** in 39% yield over the four steps (Scheme 2).

Silva et al.[4] have reported that statine-like inhibitors incorporating the (*S*)-3-methyl-2-[(1-pyridin-2-ylmethanoyl)amino]butyric acid (**B1**) in P-side and H-Ala-Leu-NH_2[20] (**A1**) in the P′-side (Scheme 3) are potent inhibitors of Plm II. These amino acid derivatives were therefore used as reference substituents for the new statine-like inhibitors.

Scheme 3[a]

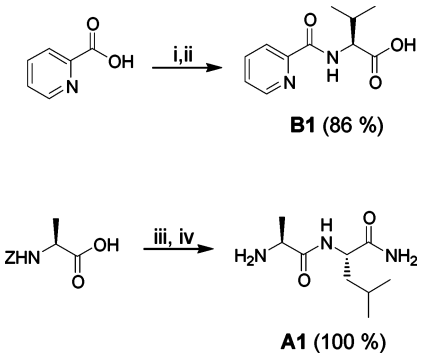

[a] Reagents and conditions: (i) H-Val-O*t*Bu·HCl, HATU, DIEA, DMF; (ii) TFA, Et_3SiH CH_2Cl_2; (iii) H-Leu-NH_2, EDC, HOAt, Proton Sponge, DMF; (iv) H_2/Pd−C, EtOH.

Scheme 4[a]

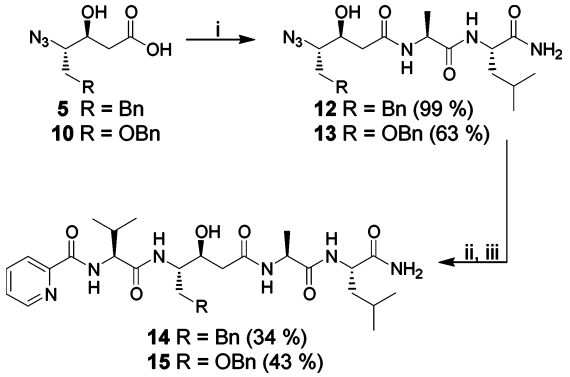

[a] Reagents and conditions: (i) **A1**, HATU, DIEA, DMF; (ii) PPh_3, MeOH, H_2O; (iii) **B1**, HATU, DIEA, DMF.

For the synthesis of **B1**, 2-picolinic acid was coupled with H-Val-O*t*Bu·HCl using *O*-(7-azabenzotriazol-1-yl)-*N,N,N′,N′*-tetramethyluronium hexafluorophosphate (HATU) and DIEA in DMF (Scheme 3). Subsequent hydrolysis of the *tert.*-butyl ester using TFA and triethylsilane in dichloromethane[21] furnished **B1** in 86% yield. For the synthesis of **A1**, Z-Ala-OH was coupled with H-Leu-NH_2 using standard coupling conditions, i.e., *N*-(3-dimethylaminopropyl)-*N′*-ethylcarbodiimide hydrochloride (EDC), 1-hydroxy-7-azabenzotriazole (HOAt), and (1,8-bis(*N,N*-dimethylamino)naphthalene (Proton Sponge) in DMF. Catalytic hydrogenation over 10% palladium on active carbon afforded **A1** in quantitative yield over the two steps.

Scheme 4 depicts the solution-phase synthesis of inhibitors **14** and **15** from scaffolds **5** and **10**. Couplings of **5** and **10** with **A1** using HATU and DIEA in DMF gave compounds **12** and **13** in 99% and 63% yields, respectively. Reduction of the azide groups with triphenylphosphine in methanol containing a few drops of water and subsequent coupling of the resulting amines with carboxylic acid **B1** employing HATU and DIEA in DMF yielded compounds **14** and **15** in 34% and 43%, respectively.

For scaffold **11** containing the *p*-bromobenzyloxy substituent a solid-phase combinatorial synthetic route was employed to obtain the target molecules. The azido hydroxyalkyl ester scaffold **11** was attached to a dihydropyran functionalized polystyrene support (loading: 1.17 mmol/g)[22] using pyridinium *p*-toluenesulfonate (PPTS) as acid catalyst in 1,2-dichloroethane at 82 °C[23]

Scheme 5[a]

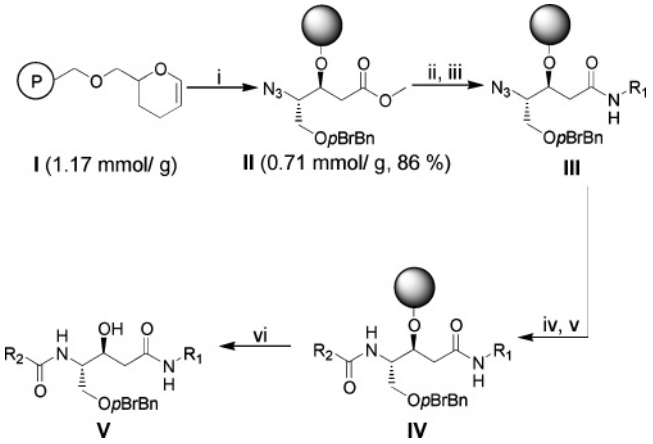

[a] Reagents and conditions: (i) **11**, PPTS, 1,2-dichloroethane; (ii) LiOH, THF/MeOH/H_2O; (iii) R_1NH_2, PyBOP, NMM DMF; (iv) $SnCl_2$, thiophenol, TEA, THF; (v) R_2COOH PyBOP, HOBt, DIEA, DMF; (vi) TFA, CH_2Cl_2, EtOH.

to give the support-bound azidoalkyl ester **II** with a loading efficiency/yield of 86% and a practical loading level of 0.71 mmol/g (Scheme 5). The loading level of the resin was estimated from the mass balance of purified recovered scaffold **11** obtained after cleavage from the solid support. The support-bound ester **II** was hydrolyzed with lithium hydroxide in THF−MeOH−H_2O and the resulting carboxylic acid was coupled to a selection of amines using (benzotriazol-1-yloxy)tripyrrolidino phosphonium hexafluoro phosphate (PyBOP) and *N*-methylmorpholine (NMM) in DMF to introduce the R_1 substituents in **III**. Trials to employ potassium trimethylsilanolate in the hydrolysis of the support-bound ester were initially made but resulted in our hands in poor or no formation of final compounds. Reduction of the azide group in **III** with tin(II) chloride, thiophenol, and triethylamine in THF[24] provided the corresponding support-bound amines which were then coupled with selected carboxylic acids using PyBOP, 1-hydroxybenzotriazole (HOBt), and diisopropylethylamine (DIEA) in DMF to introduce the R_2 substituents in **IV**. Finally, treatment of **IV** with TFA, dichloromethane and ethanol (99.5%) (2:2:1)[10c] gave the desired target compounds (**V**) in solution (Scheme 5).

When inhibitors having the carboxylic acid **B1** as the R_2 group were synthesized (Figure 3) the valine moiety of **B1** was partly racemized, due to the basic coupling conditions on solid support, giving a diastereomeric mixture of products in ratios ranging from 1.8:1 to 1.1:1 in favor of the desired isomer **B1** vs the unfavored **B2** diastereomer. The diastereomeric pairs were separated by column chromatography and both isomers were tested for their plasmepsin inhibitory properties. The yields of products in Figure 3 ranged between 8 and 23% based upon the loading of the hydroxyalkyl ester scaffold **11** to the solid-support. These modest yields can in part be attributed to the formation of diastereomers.

In Figure 4 a library with R_1 fixed to the amine **A1** is shown. These products were obtained in overall yields ranging from 10 to 42%.

The most promising small molecule substituents R_1 and R_2 from the previous two libraries were then combined in a new library to investigate the possibilities of identifying potent and low molecular weight inhibi-

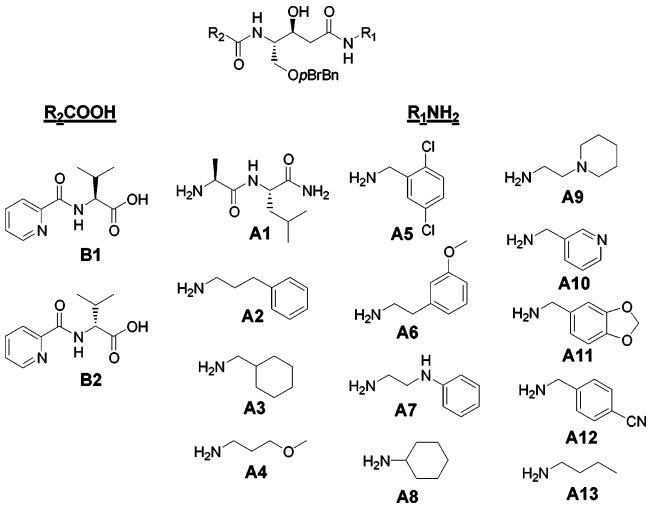

Figure 3. A library of compounds where different amines are explored as R_1 groups. R_2 is fixed to **B1** or **B2**.

tors (Figure 5). The overall yields of the products in Figure 5 were in the range of 22−40%.

Biological Data and Structure−Activity Relationships

All products were screened against both Plm I and II and inhibitors with K_i values below 60 nM are shown in Table 1 together with reference compound **A**.[4] The two most potent small molecule inhibitors, compounds **33** and **34**, are also included. Table 1 also show the total synthesis yields of the inhibitors, K_i values for the inhibition of human cathepsin D, and for selected compounds, the percentage inhibition of parasite growth in infected red blood cells (RBC) at an inhibitor concentration of 5 μM.

Plasmepsin I and II share significant homology with human cathepsin D,[5b] an aspartic peptidase with a wide tissue distribution predominantly located in the intracellular lysosomal compartments. Knockout mice lacking functional cathepsin D have a limited life span[25] indicating that high selectivity will be of critical importance in the development of anti-malarial plasmepsin inhibitor drugs.

From examination of the X-ray crystal structures of pepstatin A bound to plasmepsin II (PDB entry 1sme), it is evident that the S1 pocket extends into the S3 pocket occupied by valine in the P3 position of pepstatin A. To deliver more potent and selective drug-like plasmepsin I and II inhibitors, we have now extended the P1 substituent in the statine core to bridge from the S1 pocket into the S3 subsite.

3-D structural models of compounds **A**, **14**, **15**, and **16** (Table 1) were constructed from pepstatin A using the X-ray crystal coordinates of pepstatin A in complex with plasmepsin II (PDB entry 1sme) as a starting point. The capped Val N-terminus in pepstatin A was replaced by 2-picolinic acid, the statine *i*-butyl side chain was replaced by in turn a methylphenyl (**A**), methylbenzyl (**14**), methylbenzyloxy (**15**), and *p*-bromomethylbenzyloxy (**16**), and finally the C-terminal was replaced with H-Ala-Leu-NH_2.

These inhibitors were minimized in complex with Plm II. The residues closest to the inhibitor, within 5 Å, were allowed to move during the minimizations while the rest of the enzyme was fixed. The non-hydrogen heavy atoms in the P2, P2′, and P3′ substituents of the inhibitors were also kept fixed during the minimizations while the N-terminus 2-picolinic acid, the P1 substituent and the C-terminal amide were allowed to move.

The minimizations were performed with MINIMIZE in SYBYL 6.9, with the conjugate gradient method allowing each run for 10 000 iterations. The Tripos force field and Gasteiger−Huckel charges were used during the minimizations. All the minimizations converged before 10 000 iterations.

Modeling of Inhibitor A. The hydrophobic P1 side chain is positioned in the S1 pocket and extends slightly into the S3 pocket. The phenyl ring has close contacts with Tyr77, Ile123, Ile 32, and Phe111. The P1 phenyl also has intramolecular close stacking contacts with the 2-picolinic amide ring, which is positioned in the outer parts of the S3 pocket. The 2-picolinic amide has close contacts with Thr114 and Met15. The amide carbonyl has lost the H-bond that the corresponding carbonyl in pepstatin A makes with Ser218 main chain NH while the H-bond to Ser79 side chain OH is still there (Figure 6).

Modeling of Inhibitor 14. The P1 methylbenzyl substituent in structure **14** is less flexible than the methylbenzyloxy groups of structures **15** and **16**. This results in unfavorable steric interactions with either Phe111 or Gly216, dependent on the orientation of the phenyl ring.

Modeling of Inhibitors 15 and 16. The compounds **15** and **16** gave very similar results in the minimizations. The P1 side chain reaches through the S1 and deep into the S3 pocket as predicted. The methyl−*O*−methyl ether linkage has close contacts with Gly216, Tyr77, Ile123, and Ile 32. The phenyl ring has close contacts with Ile123, Ile32, Phe 111, Thr114, Phe120, and Met15. The phenyl ring has a favorable intramolecular stacking interaction with the 2-picolinic amide ring (Figure 7).

It is thus evident from modeling that the methyl−*O*−methyl ether linkage in structures **15** and **16** gives flexibility to the P1 substituent so that it can readily accommodate the phenyl in a suitable position in the continuous S1−S3 subsite. There are several beneficial hydrophobic close contacts of the P1 that contribute to the over all good binding properties of compounds **15** and **16**. From modeling there is no obvious advantage of the *p*-bromo substituent in inhibitor **16**. The clear loss of activity of inhibitor **14** as compared to inhibitors **A**, **15**, and **16** is likely due to the inflexibility of the ethyl linkage in **14**, forcing the phenyl group into a less advantageous positions in the S1−S3 subsite resulting in steric interactions with enzyme residues.

Compounds **14**−**24** all incorporate the picolinic amide-valine capping group R_2 (**B1**). Previously published data indicate that Plm II shows preference for β-branched carbon in the inhibitor P2 position.[9b] From molecular modeling we predict that the picolinic acid capping group only occupies the edge of the S3 pocket of Plm II, making it likely that the S1−S3 pocket should be favorably positioned to accommodate larger P1 groups than those previously explored for these type of inhibitors. Compounds **14**−**24** are potent inhibitors of both Plm I and II, indicating that this structural fragment

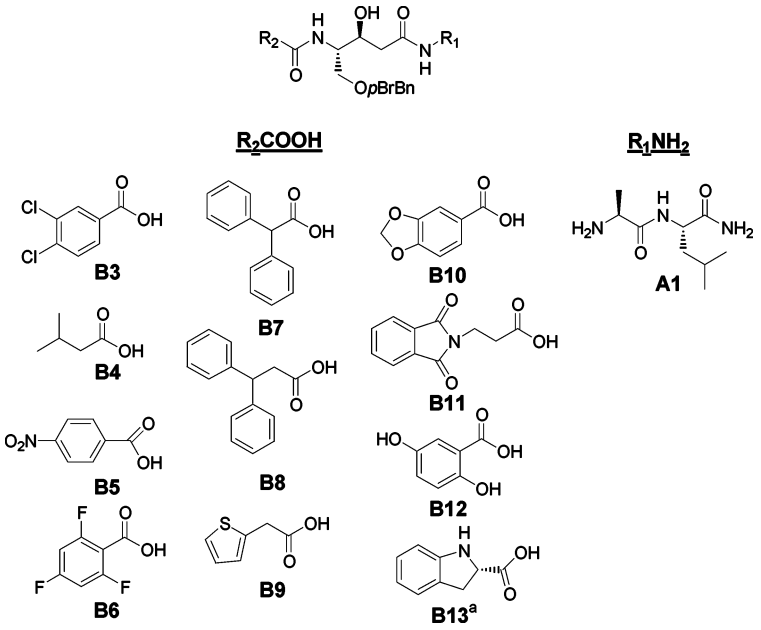

Figure 4. R_2 carboxylic acid library. R_1 is fixed to **A1**. [a]The amine functionality was Boc protected during the coupling reaction. The Boc group was removed during the acidic cleavage in the final step.

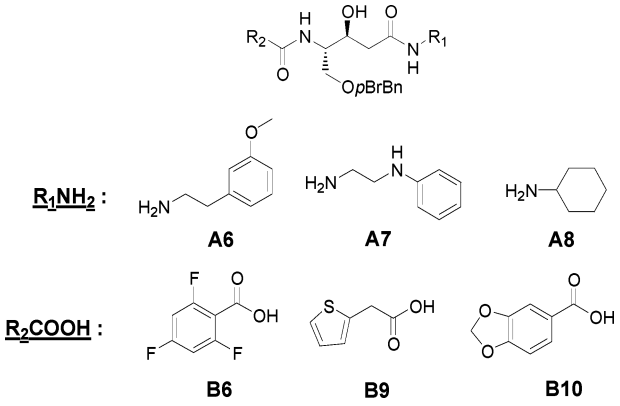

Figure 5. Target compounds combining the most promising small R_1 and R_2 groups.

indeed extends into the S3 subsite of the plasmepsins and also gives rise to favorable interactions and a good fit in the active site. Moreover, we have found that larger groups in the P1 position of these inhibitors preferentially show increased affinity toward Plm I over Plm II. While inhibitor **15** and **16** show modest selectivity toward cathepsin D with K_i values of 41 nM and 4.9 nM, respectively, inhibitor **14** shows promising selectivity with a K_i value of 980 nM. The most potent of the inhibitors incorporating the picolinic acid-valine capping group R_2 (**B1)** is compound **16**, having the H-Ala-Leu-NH_2 (**A1**) motif as the R_1 substituent, with K_i values of 0.5 nM and 2.2 nM for Plm I and II, respectively. Interestingly, compound **16** is also the most efficient inhibitor of parasite growth in vitro showing 51% inhibition at 5 μM concentration. In attempts to reduce size and peptidic characters while maintaining potency of the inhibitors the two amide groups, H-Ala-Leu-NH_2, on the P′-side were replaced by various alkyl groups. From the exemplar inhibitors **17**, **18**, **20, 21**, **22**, and **24** it can be seen that this approach holds promise with inhibitors exhibiting K_i values for Plm I below 10 nM. Compound **25** is the diastereomer of **16** having the (*R*) stereochemistry in the P2 valine moiety (a result of epimerization during the solid phase synthesis). It is approximately 10 times less potent than **16**, demonstrating the importance of (*S*) configuration in this position. However, an intriguing observation is that although compound **25** is about 10 times less potent than compound **16**, it is almost an equipotent inhibitor of parasite growth (50% at 5 μM concentration).

For compounds **26**−**32** having H-Ala-Leu-NH_2 as R_1 substituent, the picolinic amide-valine capping group R_2 (**B1**) is replaced with smaller carboxylic acid derivatives furnishing more druglike inhibitor compounds. Within this series, inhibitor **27** having 2,4,6-trifluorobenzoic acid as R_2 substituent exhibits surprisingly good K_i values of 3.4 nM and 10 nM for Plm I and II, respectively. This inhibitor also shows good selectivity toward cathepsin D (K_i > 4000 nM). High selectivity toward cathepsin D is also seen for inhibitors **27**, **33**, and **34.** It is apparent that cathepsin D selective inhibitors can be designed by reframing form utilizing the S3 binding pockets and by use of appropriate arylbenzoic acids or bulky alkyl acids as capping groups for the N-terminus of the statine-like core. From examination of the X-ray crystal structures of cathepsin D and Plamepsin II, both in complex with pepstatin A, it can be seen that amino acid Ile 290 in plasmepsin II has a larger amino acid Met 307 in the corresponding position in cathepsin D and that Leu 292 in proximity to the S2 pocket in plasmepsin II has the amino acid Met 309 in the corresponding position in cathepsin D. Moreover, the *p*-fluoro atom in compound **27** is likely pointing toward the sulfur atom of Met 307 making unfavorable interactions. This supports our observation that the S2 pocket in cathepsin D is smaller than that in plasmepsin II and that this can be used to advantage in the design of cathepsin D selective plasmepsin inhibitors.

Compounds **33** and **34** represent the two most potent of the small molecule inhibitors. They both show modest but promising activities against both Plm I and II, and inhibitor **33** inhibits parasite growth with 29% inhibition at 5 μM.

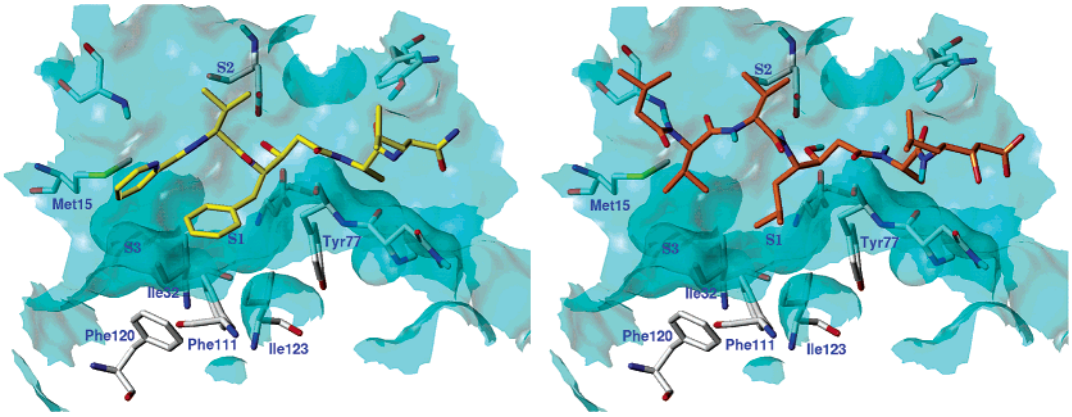

Figure 6. The active site of plasmepsin II (crystal structure PDB entry 1sme) is shown with inhibitor **A** modeled (yellow) to the left and with pepstatin A (orange) to the right.

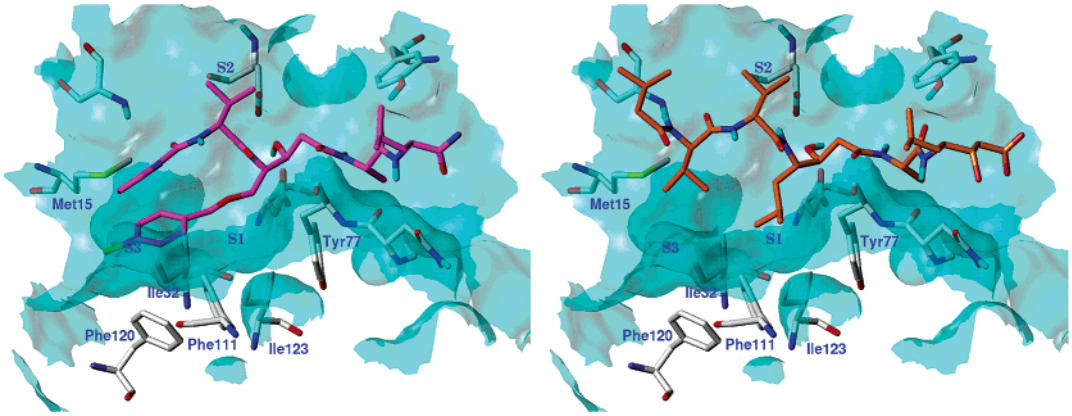

Figure 7. Inhibitor **16** (magenta) to the left is modeled into plasmepsin II (crystal structure PDB entry 1sme). The *p*-bromomethylbenzyloxy P1 group reaches through the S1 and into the S3 subsite defined by Met15, Ile32, and Phe120. Pepstatin A (orange) is shown to the right as a comparison.

Conclusion

Efficient synthetic routes with excellent stereochemical control have been developed for the key intermediates **5**, **10**, and **11** (Schemes 1 and 2). Subsequently, several directed compound libraries have been prepared utilizing solid-phase chemistry to diversify the promising *p*-bromobenzyloxy scaffold **11**. Highly potent inhibitors of Plm I and II have been identified, and several of these inhibitors show excellent cathepsin D selectivity. The X-ray crystal structure of cathepsin D and plasmepsin II and SAR analysis indicates that the observed cathepsin D selectivity is mainly attributed to the P3 and P2 substituents of the inhibitors. Moreover, it has been shown that the P1 substituent is important for achieving high Plm I inhibition with potency being favored by larger P1 groups. The most potent inhibitor in this report, compound **16**, displays K_i values of 0.5 and 2.2 nM for Plm I and II, respectively. Inhibitor **16** is also effective in attenuating parasite growth in red blood cells, showing 51% inhibition at 5 μM concentration.

Several inhibitors, i.e., **15**, **17**, **18**, **20**, **21**, **22**, **24**, **25**, and **27**, exhibit K_i values for Plm I below 10 nM. Two small molecule inhibitors, compounds **33** and **34**, show promising activities against both Plm I and II where inhibitor **33** inhibits parasite growth in red blood cells with 29% inhibition at a concentration of 5 μM.

Experimental Section

Enzyme Inhibition Measurements. Pro-plasmepsin II was a generous gift from Helena Danielson (Department of Biochemistry, Uppsala University, Uppsala, Sweden). The expression and purification of plasmepsin I will be published elsewhere.[26] Human liver cathepsin D was purchased from Sigma-Aldrich, Sweden. The activities of plasmepsin I (Plm I), plasmepsin II (Plm II) and cathepsin D was measured essentially as described previously,[3] using a total reaction volume of 100 μL. The concentration of pro-Plm II was 3 nM, the amount of Plm I was adjusted to give similar catalytic activity and 50 ng/mL pro-cathepsin D was used. The pro-sequence of Plm II was cleaved off by preincubation in assay reaction buffer (100 mM sodium acetate buffer (pH 4.5), 10% glycerol, and 0.01% Tween 20) at room temperature for 40 min, and cathepsin D was activated by incubation in the same reaction buffer at 37 °C for 20 min. The reaction was initiated by the addition of 3 μM substrate (DABCYL-Glu-Arg-Nle-Phe-Leu-Ser-Phe-Pro-EDANS, AnaSpec Inc, San Jose, CA), and hydrolysis was recorded as the increase in fluorescence intensity over a 10 min time period, during which the fluorescence increased linearly with time.

Stock solutions of inhibitors in DMSO were serially diluted in DMSO and added directly before addition of substrate, giving a final DMSO concentration of 1%.

IC_{50} values were obtained by assuming competitive inhibition and fitting a Langmuir isotherm ($v_i/v_o = 1/(1 + [I]/IC_{50})$) to the dose response data (Grafit), where v_i and v_o are the initial velocities for the inhibited and uninhibited reaction, respectively, and [I] is the inhibitor concentration.[27] The K_i

was subsequently calculated by using $K_i = IC_{50}/(1 + [S]/K_m)$[28] and a K_m value determined according to Michaelis−Menten.

***Plasmodium falciparum* Growth Inhibition Assay.** Culture and synchronization of the asexual blood stages of *Plasmodium falciparum* (clone 3D7) was performed as previously described.[29] Assays evaluating the effects of compounds on parasite growth were performed using a modification of the [^{3}H]hypoxanthine incorporation assay described by Chulay et al.[11] Briefly, a highly synchronous culture containing early trophozoite stage parasites at ∼1% haematocrit and 1% parasitaemia was supplemented with [^{3}H]hypoxanthine (Amersham Biotech) to 10 μCi ml^{-1}, and then 50 μL aliquots were dispensed into wells of flat-bottomed 96-well microtiter plates. Wells were supplemented with an equal volume of medium containing various concentrations of test compound (1−5 μM final) or DMSO only (maximum final concentration 1% v/v). Plates were transferred to gassed boxes and cultured at 37 °C for 30 h to allow parasite development through to mature schizont stage. Cultures were then harvested onto glass fiber filters (Filtermat A, Wallac, Turku, Finland) using a cell harvester. Filters were wetted with scintillation cocktail and bound radioactivity quantified in a β-counter. Control cultures containing established growth-inhibitory compounds or without parasites were included in each experiment. The amount of radioactivity in each sample was expressed relative to that in the control wells containing DMSO only. Four independent experiments were performed for each concentration of each test compound.

General Methods. NMR-spectra were recorded on a Varian 300 MHz instrument using $CDCl_3$ and CD_3OD as solvents. TMS was used as reference. Optical rotations were measured using a Perkin- Elmer 141 polarimeter. TLC was carried out on Merck precoated 60 F_{254} plates using UV-light and charring with ethanol/sulfuric acid/*p*-anisaldehyde/acetic acid 90:3:2:1, and a solution of 0.5% ninhydrin in ethanol for visualization. Flash column chromatography was performed using silica gel 60 (0.040−0.063 mm, Merck). Organic phases were dried over anhydrous magnesium sulfate. Concentrations were performed under diminished pressure (1−2 kPa) at a bath temperature of 40 °C. MALDI-TOF-spectra were recorded on a Voyager-DE STR Biospectrometry Workstation using α-cyano-4-hydroxycinnamic acid as a matrix and reference. HPLC was performed on a preparative C-18 column.

Target Molecules. All target molecules depicted in Figures 3−5 were purified by flash column chromatography or HPLC, identified by NMR and MALDI-TOF, and lyophilized from dioxane before the biological testing.

General Synthetic Procedures. Procedure A. Solid-Phase Reactions (used in the synthesis of compounds 16−34):

Preparation of the DHP-resin (I). The DHP resin was prepared according to ref 23.

Preparation of the Scaffold Loaded Resin (II). To the scaffold (**4**) (3.01 g, 8.40 mmol) dissolved in dry 1,2-dichloroethane was added the DHP-resin (**1**) (2.44 g, 1.17 mmol/g loading, 2.85 mmol). The slurry was allowed to swell in room temperature for 30 min before PPTS (2.11 g, 8.40 mmol) dissolved in dry 1,2-dichloroethane was added, and the temperature was raised to 82 °C. The mixture was shaken for 48 h, and the resin was dried and washed with DMF (4×), dichloromethane (5×), and methanol (2×). The loaded resin was dried on a high vacuum pump for 24 h to afford **II** (0.71 mmol/g loading, 86% loading efficiency) as a brown powder.

Hydrolysis of the Methyl Ester and Coupling of the Amines (III). The scaffold loaded resin (**II**) was washed twice with THF and was then allowed to swell in THF (6 mL) for 30 min. To the slurry was added a solution of lithium hydroxide (1 M in methanol/water (7:1), 2.11 mL), and the resin was shaken in room temperature for 72 h. The resin was isolated by filtration and washed with methanol/water (3:1) (3×), methanol (3×), THF (3×), THF/HOAc (8:1) (2×, rapidly), THF (3×), and methanol (3×).

The resin was then washed twice with DMF and was then allowed to swell in DMF for 30 min. Thereafter the DMF was removed and a solution of PyBOP in DMF was added to the resin followed by the amine in DMF and NMM in DMF to give total concentrations of 0.4 M in respect to PyBOP and amine and 0.8 M in respect to NMM. The slurry was shaken at room-temperature overnight before the solution was drained, and the resin was washed with DMF (5×), methanol (3×), and dichloromethane (5×).

Reduction of the Azide and Coupling of the Carboxylic Acids (IV). The resin was washed with dry THF (2×), after which it was allowed to swell in dry THF for 30 min. Solutions of tin(II) chloride, thiophenol, and triethylamine in dry THF were added to give the total concentrations of 0.2, 0.8, and 1.0 M in the reagents, respectively. The mixture was shaken at room temperature for 3 h and 15 minutes. Thereafter it was dried and washed with THF/H_2O (2:1) (2×), DMF (2×), and dichloromethane (3×).

The resin was washed twice with DMF and was allowed to swell in DMF for 30 min before the DMF was drained and a solution of the carboxylic acid, PyBOP, HOBt, and DIEA (0.2, 0.2, 0.2, 0.6 M, respectively in DMF) that had been stirred for 5 min was added. The slurry was shaken overnight after which the resin was isolated by filtration and washed with DMF (3×), dichloromethane (3×), and methanol (3×).

Cleavage of the Target Molecules from the Resin (V). A solution of TFA, dichloromethane and ethanol (99.5%) (2:2:1) was added to the resin, and the slurry was shaken at room temperature for 90 min. The solvents were collected, and the resin was washed and shaken for 5 min with dichloromethane, methanol, and dichloromethane, respectively. The solvents were pooled, evaporated, and coevaporated with toluene.

Synthetic Procedures. 3-Deoxy-1,2-*O*-isopropylidene-D-glucose (1). Compound **1** was synthesized in 68% yield over three steps according to ref 14.

5,6-Anhydro-3-deoxy-1,2-*O*-isopropylidene-D-glucose (2). To the diol **1** (2.51 g, 12.3 mmol) dissolved in chloroform (200 mL) were added triphenylphosphine (3.87 g, 14.8 mmol) and diisopropyl azodicarboxylate (DIAD) (2.90 mL, 15.0 mmol), and the mixture was refluxed overnight. The solvent was evaporated and purification by flash column chromatography (toluene/ethyl acetate 15:1) yielded **2** (1.57 g, 69%) as a colorless oil. **2**: Analytical data in accordance with ref 16.

6-Benzyl-3,6-dideoxy-1,2-*O*-isopropylidene-D-glucose (3). Compound **2** (0.73 g, 3.90 mmol) was dissolved in dry tetrahydrofuran (70 mL) and the temperature was lowered to 0 °C. Benzylmagnesium chloride (1.3 M in THF) (24.0 mL, 31.2 mmol) was added and the mixture was allowed to attain room temperature and was then stirred overnight. The reaction was quenched by the addition of water and the THF was evaporated. The water phase was extracted three times with ethyl acetate and the combined organic phases were dried, filtered and concentrated. The crude product was purified by flash column chromatography (gradient elution from toluene/ethyl acetate 15:1 to 2:1) to give **3** (1.08 g, 100%) as yellow-white solid. **3**: $[\alpha]^{22}_D$ −6.9 (*c* 0.6, $CHCl_3$); ^{1}H NMR (CD_3OD, 300 MHz) δ 1.28 (s, 3H), 1.44 (s, 3H), 1.53−1.69 (m, 1H), 1.70−1.86 (m, 2H), 1.99 (dd, J = 4.5, 13.3 Hz, 1H), 2.58−2.72 (m, 1H), 2.79−2.92 (m, 1H), 3.63−3.72 (m, 1H), 4.03−4.14 (m, 1H), 4.64−4.71 (m, 1H), 5.75 (d, J = 3.6 Hz, 1H), 7.10−7.29 (m, 5H); ^{13}C NMR (CD_3OD, 75.5 MHz) δ 26.5, 27.2, 32.8, 34.0, 36.2, 71.6, 81.6, 82.4, 106.5, 111.9, 126.6, 129.2, 129.3, 143.1. Anal. ($C_{16}H_{22}O_4$) C, H.

5-Azido-6-benzyl-1,2-*O*-isopropylidene-3,5,6-trideoxy-L-idose (4). Compound **3** (1.06 g, 3.81 mmol) and triphenylphosphine (1.51 g, 5.75 mmol) were dissolved in dry THF (14 mL). Thereafter the mixture was cooled to −15 °C, and diisopropyl azodicarboxylate (DIAD) (1.90 mL, 9.65 mmol) was added. The mixture was stirred for 10 min at −15 °C, the temperature was raised to 0 °C, and diphenylphosphoryl azide (DPPA) (1.25 mL, 5.78 mmol) was added. After stirring for 30 min at 0 °C, the reaction mixture was allowed to attain room temperature and was stirred overnight. The solvent was evaporated and the crude material was purified by flash column chromatography (toluene) yielding the azide (**4**) (1.06 g, 92%). **4**: $[\alpha]^{22}_D$ −67.8 (*c* 0.7, $CHCl_3$); ^{1}H NMR (CD_3OD, 300

MHz) δ 1.28 (s, 3H), 1.45 (s, 3H), 1.62−1.74 (m, 1H), 1.76−1.86 (m, 2H), 2.00 (dd, J = 4.5, 13.3 Hz, 1H), 2.62−2.73 (m, 1H), 2.75−2.86 (m, 1H), 3.08−3.17 (m, 1H), 4.15−4.24 (m, 1H), 4.68−4.74 (m, 1H), 5.77 (d, J = 3.6 Hz, 1H), 7.13−7.30 (m, 5H); ^{13}C NMR (CD_3OD, 75.5 MHz) δ 26.4, 27.1, 33.2, 33.7, 36.7, 64.9, 81.6, 82.0, 106.8, 112.4, 127.1, 129.4, 129.5, 142.3. Anal. ($C_{16}H_{21}N_3O_3$) C, H, N.

(3*S*,4*S*)-4-Azido-3-hydroxy-6-phenylhexanoic Acid (5). Compound **4** (1.04 g, 3.43 mmol) was dissolved in acetic acid/water (1:1, 26 mL) and was allowed to reflux for 1 h. Thereafter the solvent was evaporated, the crude product was dissolved in *tert*-butyl alcohol/water (2:3, 25 mL), and sodium periodate (3.68 g, 17.2 mmol) was added. After the mixture was stirred at room temperature for 15 min, potassium permanganate (0.076 g, 0.48 mmol) was added and the mixture was stirred at room temperature for an additional 1 h. The reaction mixture was extracted three times with chloroform after which the organic phases were pooled, washed once with brine, dried, filtered, and concentrated.

The crude material was dissolved in water/dioxane 3:1 (40 mL), and the mixture was cooled to 0 °C. Sodium hydroxide (0.55 g, 13.7 mmol) in water (19 mL) was added dropwise at 0 °C after which the mixture was stirred in room temperature for 1 h. The water phase was washed twice with diethyl ether and was then acidified with 6 M hydrochloric acid to pH 1−2. The acidified water phase was extracted three times with chloroform, and the combined organic phases were evaporated. The crude material was purified by flash column chromatography (toluene/ethyl acetate 2:1 + 1% HOAc) to give **5** (0.54 g, 64%) as yellow oil. **5**: $[\alpha]^{22}_D$ −25.8 (c 0.7, MeOH); ^{1}H NMR (CD_3OD, 300 MHz) δ 1.88−1.99 (m, 2H), 2.52 (d, J = 6.9 Hz, 2H), 2.64−2.83 (m, 2H), 3.13−3.22 (m, 1H), 4.03−4.13 (m, 1H), 7.11−7.25 (m, 5H); ^{13}C NMR (CD_3OD, 75.5 MHz) δ 33.2, 33.4, 39.9, 66.2, 71.4, 127.0, 129.5, 142.4, 174.9. Anal. ($C_{12}H_{15}N_3O_3$) C, H, N.

6-Benzyloxy-3-deoxy-1,2-*O*-isopropylidene-D-glucose (6). Compound **1** (3.00 g, 14.7 mmol) and dibutyl tin oxide (4.84 g, 19.4 mmol) was dissolved in toluene (90 mL). The mixture was refluxed for 5 h after which the temperature was lowered to 90 °C and tetrabutylammonium bromide (TBAB) (6.27 g, 19.4 mmol) and benzyl bromide (2.21 mL, 18.6 mmol) were added. The mixture was allowed to stir at 90 °C overnight, and thereafter the solvent was evaporated and the crude product was purified by flash column chromatography (toluene/ethyl acetate 2:1) to give **6** (4.06 g, 94%) as a colorless solid. **6**: $[\alpha]^{22}_D$ −10.2 (c 0.6, $CHCl_3$); ^{1}H NMR ($CDCl_3$ 300 MHz): δ 1.32 (s, 3H), 1.50 (s, 3H), 1.78−1.91 (m, 1H), 2.06 (dd, J = 4.4, 13.5 Hz, 1H), 3.48 (dd, J = 6.3, 9.9 Hz, 1H), 3.59 (dd, J = 3.9, 9.9 Hz, 1H), 3.96−4.03 (m, 1H), 4.18−4.28 (m, 1H), 4.54 (d, J = 12.1 Hz, 1H), 4.58 (d, J = 12.1 Hz, 1H), 4.73 (app. t, J = 3.9 Hz, 1H), 5.79 (d, J = 3.9 Hz, 1H), 7.27−7.38 (m, 5H). ^{13}C NMR ($CDCl_3$, 75.5 MHz): δ 26.2, 26.8, 33.9, 71.0, 71.3, 73.5, 78.4, 80.6, 105.4, 111.3, 127.8, 127.9, 128.5, 137.8. Anal. ($C_{16}H_{22}O_5$) C, H.

6-(4-Bromobenzyloxy)-3-deoxy-1,2-*O*-isopropylidene-D-glucose (7). Compound **7** was prepared in 100% yield (colorless solid) according to the method for the preparation of compound **6** using 4-bromobenzyl bromide. **7**: $[\alpha]^{22}_D$ −8.4 (c 0.8, $CHCl_3$); ^{1}H NMR ($CDCl_3$ 300 MHz): δ 1.32 (s, 3H), 1.50 (s, 3H), 1.73−1.85 (m, 1H), 2.06 (dd, J = 4.4, 13.5 Hz, 1H), 3.46 (dd, J = 6.6, 9.6 Hz, 1H), 3.57 (dd, J = 3.9, 9.9 Hz, 1H), 3.89−3.97 (m, 1H), 4.16−4.25 (m, 1H), 4.49 (s, 2H), 4.72 (t, J = 4.3 Hz, 1H), 5.78 (d, J = 3.9 Hz, 1H), 7.19 (d, J = 8.3 Hz, 2H), 7.46 (d, J = 8.3 Hz, 2H).^{13}C NMR ($CDCl_3$, 75.5 MHz): δ 25.8, 26.5, 33.5, 70.5, 72.0, 78.1, 78.2, 79.7, 105.0, 110.8, 121.2, 129.0, 129.0, 131.1, 131.1, 136.7. Anal. ($C_{16}H_{21}BrO_5$) C, H.

5-Azido-6-benzyloxy-3,5-dideoxy-1,2-*O*-isopropylidene-L-idose (8). Compound **6** (4.01 g, 13.6 mmol) and triphenylphosphine (4.65 g, 17.7 mmol) were dissolved in dry THF (50 mL). Thereafter the mixture was cooled to −15 °C, and diisopropyl azodicarboxylate (DIAD) (5.70 mL, 29.0 mmol) was added. The mixture was stirred for 10 min at −15 °C, the temperature was raised to 0 °C, and diphenylphosphoryl azide (DPPA) (3.93 mL, 18.5 mmol) was added. After being stirred for 30 min at 0 °C, the reaction mixture was allowed to attain room temperature and was stirred overnight. The solvent was evaporated, and the crude product was purified by flash column chromatography (toluene/ethyl acetate 24:1) yielding the azide (**8**) (4.35 g, 100%). **8**: $[\alpha]^{22}_D$ −5.3 (c 0.9, $CHCl_3$); ^{1}H NMR ($CDCl_3$, 300 MHz): δ 1.30 (s, 3H), 1.49 (s, 3H), 1.79−1.92 (m, 1H), 2.04 (dd, J = 4.7, 13.5 Hz, 1H), 3.48−3.56 (m, 1H), 3.67−3.75 (m, 2H), 4.27−4.35 (m, 1H), 4.57 (s, 2H), 4.68−4.75 (m, 1H), 5.79 (d, J = 3.6 Hz, 1H), 726−7.38 (m, 5H). ^{13}C NMR ($CDCl_3$, 75.5 MHz): δ 26.2, 26.8, 35.4, 62.6, 70.5, 73.6, 77.4, 80.3, 105.5, 111.5, 127.7, 127.9, 128.5, 137.6. Anal. ($C_{16}H_{21}N_3O_4$) C, H, N.

5-Azido-6-(4-bromobenzyloxy)-3,5-dideoxy-1,2-*O*-isopropylidene-L-idose (9). Compound **9** was synthesized in 100% yield from **7** according to the method for the preparation of compound **8**. **9**: $[\alpha]^{22}_D$ −2.6 (c 0.5, $CHCl_3$); ^{1}H NMR ($CDCl_3$, 300 MHz): δ 1.30 (s, 3H), 1.49 (s, 3H), 1.82−1.93 (m, 1H), 2.04 (dd, J = 4.7, 13.5 Hz, 1H), 3.49−3.57 (m, 1H), 3.66−3.75 (m, 2H), 4.30 (dt, J = 4.4, 10.4 Hz, 1H), 4.57 (s, 2H), 4.71 (dd, J = 4.1, 8.2 Hz, 1H), 5.79 (d, J = 3.6 Hz, 1H), 7.20 (d, J = 8.5 Hz, 2H), 7.47 (d, J = 8.5 Hz, 2H). ^{13}C NMR ($CDCl_3$, 75.5 MHz): δ 26.4, 27.0, 34.7, 35.6, 62.8, 70.8, 72.7, 77.5, 80.4, 105.7, 121.9, 129.5, 129.7, 131.7, 131.8, 137.0. Anal. ($C_{16}H_{20}BrN_3O_4$) C, H, N.

(3*S*,4*S*)-4-Azido-5-benzyloxy-3-hydroxypentanoic Acid (10). Compound **8** (4.30 g, 13.5 mmol) was dissolved in acetic acid/water (1:1, 100 mL), and the mixture was heated to reflux for 1 h. Thereafter the solvent was evaporated crude product was dissolved in *tert*-butyl alcohol/water (2:3, 100 mL), and sodium periodate (14.40 g, 67.3 mmol) was added. The reaction mixture was allowed to stir at room temperature for 15 min before potassium permanganate (0.300 g, 1.90 mmol) was added, and the mixture was stirred for an additional 1 h. The reaction mixture was extracted three times with chloroform after which the organic phases were pooled, washed once with brine, dried, filtered, and concentrated.

The crude material was dissolved in water (110 mL), and the mixture was cooled to 0 °C. Sodium hydroxide (2.16 g, 54.0 mmol) in water (67 mL) was added dropwise at 0 °C after which the mixture was stirred in room temperature for 1 h. The water phase was washed twice with diethyl ether and was then acidified with 6 M hydrochloric acid to pH 1−2. The acidified water phase was extracted three times with chloroform, and the combined organic phases were evaporated. Purification by flash column chromatography (toluene/ethyl acetate 2:1 + 1% HOAc) provided **10** (2.13 g, 60%) as a colorless solid. **10**: $[\alpha]^{22}_D$ 8.2 (c 1.3, $CHCl_3$); ^{1}H NMR ($CDCl_3$, 300 MHz): δ 2.55 (dd, J = 4.4, 16.5 Hz, 1H), 2.67 (dd, J = 8.2, 16.5 Hz, 1H), 3.48−3.56 (m, 1H), 3.69−3.79 (m, 2H), 4.15−4.24 (m, 1H), 4.55 (s, 2H), 7.27−7.38 (m, 5H). ^{13}C NMR ($CDCl_3$, 75.5 MHz): δ 38.3, 63.7, 68.2, 70.2, 73.7, 127.8, 128.0, 128.6, 137.2, 177.0. Anal. ($C_{12}H_{15}N_3O_4 \cdot 0.20$ HOAc) C, H, N.

(3*S*,4*S*)-4-Azido-5-(4-bromobenzyloxy)-3-hydroxypentanoic Acid Methyl Ester (11). Compound **11** was synthesized from **9** in 39% yield according to the method for the preparation of compound **10** except that the crude carboxylic acid obtained in the last step was dissolved in methanol (100 mL) at 0 °C, and acetyl chloride (9 mL) was added in order to form the methyl ester. The solution was stirred for 20 min at 0 °C and for an additional 48 h at room temperature. The solvent was evaporated and coevaporated with toluene. Purification by flash column chromatography (toluene/ethyl acetate 4:1) provided **11** as a slightly yellow solid. **11**: $[\alpha]^{22}_D$ −11.5 (c 1.0, $CHCl_3$); ^{1}H NMR ($CDCl_3$, 300 MHz): δ 2.53 (dd, J = 4.4, 16.5 Hz, 1H), 2.63 (dd, J = 8.4, 16.5 Hz, 1H), 3.19−3.27 (b, 1H), 3.50−3.58 (m, 1H), 3.69 (s, 3H), 3.72−3.80 (m, 1H), 4.13−4.22 (m, 1H), 4.51 (s, 2H), 7.19 (d, J = 8.2 Hz, 2H), 7.46 (d, J = 8.2 Hz, 2H). ^{13}C NMR ($CDCl_3$, 75.5 MHz): δ 38.3, 51.9, 64.0, 68.1, 70.4, 72.7, 121.7, 125.3, 129.3, 129.6, 131.6, 136.6, 172.3. Anal. ($C_{13}H_{16}BrN_3O_4$) C, H, N.

(*S*)-3-Methyl-2-[(1-pyridin-2-ylmethanoyl)amino]butyric Acid (B1). 2-Picolinic acid (0.332 g, 2.70 mmol), H-Val-O*t*Bu×HCl (0.566 g, 2.70 mmol), and diisopropylethylamine (DIEA) (1.05 g, 8.10 mmol) were dissolved in DMF (5 mL),

and the temperature was lowered to 0 °C. Thereafter *O*-(7-azabenzotriazol-1-yl)-*N,N,N′,N′*-tetramethyluronium hexafluorophosphate (HATU) (1.03 g, 2.70 mmol) was added, and the reaction mixture was stirred for 0.5 h at 0 °C and then for an additional 1 h at room temperature. The solvent was evaporated, the crude mixture was extracted with ethyl acetate and washed twice with brine, and the organic phase was dried, filtered, and concentrated. The crude material was filtered through a short silica plug and was eluated with toluene/ethyl acetate 2:1, and the solvents were evaporated. The remainder was dissolved in dichloromethane (13 mL). Triethylsilane (0.785 g, 6.75 mmol) and trifluoroacetic acid (6.5 mL) were added, and the reaction mixture was allowed to stir in room temperature for 3 h. The solvents were evaporated and coevaporated with toluene, and the crude material was purified by flash column chromatography (toluene/ethyl acetate 2:1 + 1% acetic acid) to give compound **B1** (0.516 g, 86%) as a white powder. **B1**: $[\alpha]^{22}_D$ 38.5 (*c* 1.1, MeOH); ^{1}H NMR (CD_3OD, 300 MHz) δ 1.02 (d, J = 6.9 Hz, 6H), 2.25−2.32 (m, 1H), 4.56 (d, J = 5.2 Hz, 1H), 7.57 (ddd, J = 1.1, 4.7, 7.7 Hz, 1H), 7.97 (ddd, J = 1.7, 7.7, 8.0 Hz, 1H), 8.10 (d, J = 8.0 Hz, 1H), 8.65 (d, J = 4.7 Hz, 1H); ^{13}C NMR (CD_3OD, 75.5 MHz) δ 18.1, 19.6, 32.4, 58.8, 123.2, 128.0, 138.9, 149.8, 150.4, 166.2, 174.3. Anal. ($C_{11}H_{14}N_2O_3$) C, H, N.

(*S*)-2-((*S*)-2-Aminopropanoylamino)-4-methylpentanoic Acid Amide (A1). (Benzyloxy)carbonyl-protected alanine (Z-Ala-OH) (0.200 g, 0.90 mmol), leucine amide (H-Leu-NH_2) (0.123 g, 0.94 mmol), 1-hydroxy-7-azabenzotriazole (HOAt) (0.122 g, 0.90 mmol), and (1,8-bis(*N,N*-dimethylamino)naphthalene (Proton sponge) (0.192 g, 0.90 mmol) were dissolved in DMF (2 mL). The reaction mixture was cooled to 0 °C, and *N*-(3-dimethylaminopropyl)-*N′*-ethylcarbodiimide hydrochloride (EDC) (0.189 g, 0.99 mmol) was added. The mixture was stirred at 0 °C for 2 h and then at room-temperature overnight. The solvent was removed after which the crude mixture was extracted with chloroform and washed with brine. The solvent was evaporated, and the crude product was dissolved in ethanol (95%, 15 mL). Palladium (10%) on active carbon (∼25 mg) and hydrogen (atmospheric pressure, with flushing) were added, and the mixture was stirred for 90 min. The suspension was filtered trough Celite followed by evaporation of the ethanol, and the crude product was purified by flash column chromatography (ethyl acetate/methanol 9:1 + 1% TEA) providing **A1** (181 mg, 100%) as a white powder. **A1**: $[\alpha]^{22}_D$ −10.2 (*c* 0.5, MeOH); ^{1}H NMR (CD_3OD, 300 MHz) δ 0.94 (d, J = 6.3 Hz, 3H), 0.97 (d, J = 6.3 Hz, 3H), 1.30 (d, J = 6.9 Hz, 3H), 1.50−1.78 (m, 3H), 3.46 (q, J = 6.9 Hz, 1H), 4.41 (dd, J = 6.3, 8.5 Hz, 1H); ^{13}C NMR (CD_3OD, 75.5 MHz) δ 21.4, 22.0, 23.5, 25.9, 42.3, 51.5, 52.6, 177.5, 178.1. Anal. ($C_9H_{19}N_3O_2$·0.47MeOH) C, H, N.

(3*S*,4*S*)-4-Azido-3-hydroxy-6-phenylhexanoic Acid [(*S*)-1-((*S*)-1-Carbamoyl-3-methylbutylcarbamoyl)ethyl]-amide (12). Compound **5** (100 mg, 0.401 mmol) was dissolved in DMF (3 mL) after which **A1** (122 mg, 0.606 mmol) and DIEA (210 μL, 1.21 mmol) were added, and the temperature was lowered to 0 °C. HATU (161 mg, 0.423 mmol) was added, and reaction was stirred for 30 min at 0 °C and then at room temperature for 90 min. The solvent was evaporated, and the residual was extracted with EtOAc and washed with brine (3 ×). The aqueous phase was extracted with EtOAc, and the combined organic phases were dried over magnesium sulfate, filtered, and concentrated. The crude product was purified by flash column chromatography (ethyl acetate/methanol 4:1 + 1% TEA) yielding **12** (172 mg, 99%) as a colorless solid. **12**: $[\alpha]^{22}_D$ −51.6 (*c* 0.4, MeOH); ^{1}H NMR (CD_3OD, 300 MHz) δ 0.91 (d, J = 6.0 Hz, 3H), 0.95 (d, J = 6.3 Hz, 3H), 1.36 (d, J = 7.1 Hz, 3H), 1.55−1.75 (m, 3H), 1.86−1.99 (m, 2H), 2.43−2.55 (m, 2H), 2.66−2.83 (m, 2H), 3.18−3.27 (m, 1H), 4.04−4.12 (m, 1H), 4.29−4.43 (m, 2H), 7.14−7.31 (m, 5H); ^{13}C NMR (CD_3OD, 75.5 MHz) δ 17.7, 21.8, 23.5, 25.9, 33.3, 33.4, 41.2, 41.8, 50.8, 52.8, 66.6, 71.9, 127.1, 129.4, 129.5, 142.5, 173.8, 175.0 177.4. Anal. ($C_{21}H_{32}N_6O_4$) C, H, N.

(3*S*,4*S*)-4-Azido-5-benzyloxy-3-hydroxypentanoic Acid [(*S*)-1-((*S*)-1-Carbamoyl-3-methylbutylcarbamoyl)ethyl]-amide (13). Compound **13** was synthesized in 63% yield from **10** according to the method for the preparation of compound **12**. **13**: $[\alpha]^{22}_D$ −31.2 (*c* 0.7, MeOH); ^{1}H NMR (CD_3OD, 300 MHz) δ 0.90 (d, J = 6.3 Hz, 3H), 0.94 (d, J = 6.0 Hz, 3H), 1.36 (d, J = 7.1 Hz, 3H), 1.56−1.74 (m, 3H), 2.50 (app. d, J = 6.6 Hz, 2H), 3.01 (app. q, J = 7.4 Hz, 1H), 3.57−3.66 (m, 1H), 3.69−3.78 (m, 2H), 4.10−4.18 (m, 1H), 4.32−4.41 (m, 1H), 4.54 (d, J = 12.1 Hz, 1H), 4.59 (d, J = 12.1 Hz, 1H), 7.24−7.39 (m, 5H); ^{13}C NMR (CD_3OD, 75.5 MHz) δ 17.7, 21.8, 23.5, 25.9, 41.1, 41.8, 50.8, 52.8, 66.1, 69.4, 71.3, 74.2,128.7, 128.8, 129.3, 129.4, 139.2, 173.5, 175.0, 177.4. Anal. ($C_{21}H_{32}N_6O_5$) C, H, N.

Pyridine-2-carboxylic Acid ((*S*)-1-{(1*S*,2*S*)-3-[(*S*)-1-((*S*)-1-Carbamoyl-3-methylbutylcarbamoyl)ethylcarbamoyl]-2-hydroxy-1-phenethylpropylcarbamoyl}-2-methylpropyl)amide (14). Compound **12** (150 mg, 0.347 mmol) was dissolved in 18 mL of MeOH. Triphenylphosphine (134 mg, 0.511 mmol) and three drops of water were added, and the solution was stirred at room-temperature overnight. The solvent was evaporated, and the crude material was run through a short silica column using ethyl acetate/methanol 9:1 + 1% TEA as eluent. The crude amine was dissolved in DMF (10 mL) after which **B1** (100 mg, 0.451 mmol) and DIEA (181 μL, 1.04 mmol) were added, and the temperature was lowered to 0 °C. HATU (172 mg, 0.451 mmol) was added, and the reaction was stirred for 30 min at 0 °C and then for an additional 3 h at room temperature. The solvent was evaporated, and the residual was extracted with chloroform and washed with brine. The organic phase was dried over magnesium sulfate, filtered, and concentrated. The crude product was purified by flash column chromatography (chloroform/ethanol 13:1 + 1.5% methanol saturated with NH_3) yielding **14** (72 mg, 34%) as a slightly yellow solid. **14**: $[\alpha]^{22}_D$ −33.9 (*c* 0.3, $CHCl_3$); ^{1}H NMR (CD_3OD, 300 MHz) δ 0.89 (d, J = 6.0 Hz, 3H), 0.93 (d, J = 6.1 Hz, 3H), 1.09 (d, J = 4.4 Hz, 3H), 1.11 (d, J = 4.4 Hz, 3H), 1.41 (d, J = 7.4 Hz, 3H), 1.65−1.83 (m, 3H), 1.84−1.98 (m, 2H), 2.26−2.37 (m, 1H), 2.40 (app. d, J = 7.1 Hz, 2H), 2.50−2.70 (m, 2H), 3.89−3.99 (m, 1H), 4.09−4.17 (m, 1H), 4.19 (q, J = 7.4 Hz, 1H), 4.37−4.46 (m, 2H), 7.08−7.23 (m, 5H), 7.55−7.63 (m, 1H), 7.94−8.02 (m, 1H), 8.15 (d, J = 7.7 Hz, 1H), 8.67 (d, J = 4.7 Hz, 1H); ^{13}C NMR (CD_3OD, 75.5 MHz) δ 17.6, 18.9, 20.3, 21.5, 23.6, 26.1, 32.1, 33.8, 34.9, 40.9, 41.0, 52.0, 53.0, 53.8, 61.2, 71.1, 123.3, 126.8, 128.1, 129.3, 129.4, 139.0, 143.1, 149.9, 150.5, 166.8, 173.8, 174.4, 175.7, 177.8. Anal. ($C_{32}H_{46}N_6O_6$) C, H, N.

Pyridine-2-carboxylic Acid ((*S*)-1-{(1*S*,2*S*)-1-Benzyloxymethyl-3-[(*S*)-1-((*S*)-1-carbamoyl-3-methylbutylcarbamoyl)ethylcarbamoyl]-2-hydroxypropylcarbamoyl}-2-methylpropyl)amide15. Compound **15** was synthesized in 43% yield from **13** according to the method for the preparation of compound **14**. **15**: $[\alpha]^{22}_D$ −20.4 (*c* 0.2, $CHCl_3$); ^{1}H NMR (CD_3OD, 300 MHz) δ 0.87 (d, J = 6.3 Hz, 3H), 0.90 (d, J = 6.0 Hz, 3H), 1.03 (d, J = 6.9 Hz, 3H), 1.05 (d, J = 6.9 Hz, 3H), 1.59−1.82 (m, 3H), 2.22−2.35 (m, 1H), 2.42 (app. d, J = 7.4 Hz, 2H), 3.63 (app. d, J = 6.3 Hz, 2H), 4.14−4.30 (m, 3H), 4.35−4.51 (m, 4H), 7.16−7.32 (m, 5H), 7.54−7.61 (m, 1H), 7.93−8.03 (m, 1H), 8.13 (d, J = 8.0 Hz, 1H), 8.66 (d, J = 4.7 Hz, 1H); ^{13}C NMR (CD_3OD, 75.5 MHz) δ 17.6, 18.7, 20.1, 21.5, 23.6, 26.1, 32.2, 41.0, 41.1, 52.0, 53.1, 53.2, 61.1, 68.8, 71.1, 74.0, 123.3, 128.1, 128.5, 128.8, 129.2, 138.9, 139.5, 149.9, 150.4, 166.7, 173.9, 174.2, 175.7, 177.8. Anal. ($C_{32}H_{46}N_6O_7$) C, H, N.

Pyridine-2-carboxylic Acid ((*S*)-1-{(1*S*,2*S*)-1-(4-Bromobenzyloxymethyl)-3-[(*S*)-1-((*S*)-1-carbamoyl-3-methylbutylcarbamoyl)ethylcarbamoyl]-2-hydroxypropylcarbamoyl}-2-methylpropyl)amide (16). Synthesized according to Procedure A. Purification by column chromatography using chloroform/ethanol 13:1 + 1.5% methanol saturated with NH_3 gave **16** in 20% yield. **16**: ^{1}H NMR (CD_3OD, 300 MHz) δ 0.87 (d, J = 6.3 Hz, 3H), 0.90 (d, J = 6.1 Hz, 3H), 1.03 (d, J = 4.4 Hz, 3H), 1.05 (d, J = 4.4 Hz, 3H), 1.41 (d, J = 7.4 Hz, 3H), 1.59−1.82 (m, 3H), 2.21−2.33 (m, 1H), 2.43 (app. d, J = 7.4 Hz, 2H), 3.63 (app. d, J = 6.9 Hz, 2H), 4.13−2.28 (m, 3H), 4.36−4.49 (m, 4H), 7.17 (d, J = 8.5 Hz, 2H), 7.33 (d, J = 8.5 Hz, 2H), 7.54−7.62 (m, 1H), 7.92−8.03 (m, 1H), 8.12 (d, J =

7.7 Hz, 1H), 8.65 (d, J = 4.7 Hz, 1H); HRMS calcd for $C_{32}H_{45}BrN_6O_7Na$ $(M + Na)^+$: 727.2431. Found: 727.2402.

Pyridine-2-carboxylic Acid {(*S*)-1-[(1*S*,2*S*)-1-(4-bromobenzyloxymethyl)-2-hydroxy-3-(3-phenylpropylcarbamoyl)propylcarbamoyl]-2-methylpropyl}amide (17). Synthesized according to Procedure A. Purification by column chromatography was performed using chloroform + 1.5% methanol saturated with NH_3 giving **17** in 21% yield. **17**: ^{1}H NMR (CD_3OD, 300 MHz) δ 1.02 (d, J = 6.9 Hz, 3H), 1.06 (d, J = 6.6 Hz, 3H), 1.76−1.89 (m, 2H), 2.19−2.31 (m, 1H), 2.33 (app. d, J = 7.2 Hz, 2H), 2.65 (t, J = 7.7 Hz, 2H), 3.21 (t, J = 7.0 Hz, 2H) 3.51−3.69 (m, 2H), 4.11−4.19 (m, 1H), 4.20−4.29 (m, 1H), 4.40−4.53 (m, 3H), 7.10−7.29 (m, 7H), 7.33 (d, J = 8.5 Hz, 2H), 7.52−7.61 (m, 1H), 7.91−8.01 (m, 1H), 8.09 (d, J = 8.0 Hz, 1H), 8.65 (d, J = 4.7 Hz, 1H); HRMS calcd for $C_{32}H_{39}BrN_4O_5Na$ $(M + Na)^+$: 661.2002. Found: 661.2003.

Pyridine-2-carboxylic Acid {(*S*)-1-[(1*S*,2*S*)-1-(4-Bromobenzyloxymethyl)-3-(cyclohexylmethylcarbamoyl)-2-hydroxypropylcarbamoyl]-2-methylpropyl}amide (18). Synthesized according to Procedure A. Purification by column chromatography was performed using chloroform + 1.5% methanol saturated with NH_3 giving **18** in 15% yield. **18**: ^{1}H NMR ($CDCl_3$, 300 MHz) δ 0.84−1.00 (m, 2H), 1.03 (d, J = 7.1 Hz, 3H), 1.06 (d, J = 7.2 Hz, 3H), 1.10−1.35 (m, 3H), 1.37−1.53 (m, 1H), 1.59−1.79 (m, 6H), 2.22 (dd, J = 4.1, 14.8 Hz, 1H), 2.32−2.49 (m, 2H), 3.09 (t, J = 6.3 Hz, 2H), 3.61 (app. d, J = 5.5 Hz, 2H), 4.01−4.12 (m, 1H), 4.26−4.34 (m, 1H), 4.36−4.50 (m, 3H), 6.14−6.24 (b, 1H), 6.55−6.64 (b, 1H), 7.13 (d, J = 8.2 Hz, 2H), 7.40 (d, J = 8.2 Hz, 2H), 7.43−7.52 (m, 1H), 7.82−7.91 (m, 1H), 8.15 (d, J = 7.7 Hz, 1H), 8.48−8.54 (b, 1H), 8.59 (d, J = 4.1 Hz, 1H); HRMS calcd for $C_{30}H_{41}BrN_4O_5Na$ $(M + Na)^+$: 639.2158. Found: 639.2178.

Pyridine-2-carboxylic Acid {(*S*)-1-[(1*S*,2*S*)-1-(4-Bromobenzyloxymethyl)-2-hydroxy-3-(3-methoxypropylcarbamoyl)propylcarbamoyl]-2-methylpropyl}amide (19). Synthesized according to Procedure A. Purification by column chromatography was performed using chloroform/ethanol 40:1 + 1% triethylamine giving **19** in 15% yield. **19**: ^{1}H NMR (CD_3OD, 300 MHz) δ 1.01 (d, J = 6.8 Hz, 3H), 1.05 (d, J = 6.9 Hz, 3H), 1.69−1.81 (m, 2H), 2.18−2.30 (m, 1H), 2.32 (app. d, J = 7.1 Hz, 2H), 3.25 (t, J = 6.9 Hz, 2H), 3.30 (s, 3H), 3.43 (t, J = 6.3 Hz, 2H), 3.51−3.68 (m, 2H), 4.08−4.18 (m, 1H), 4.09−4.25 (m, 1H), 4.39−4.53 (m, 3H), 7.19 (d, J = 8.2 Hz, 2H), 7.34 (d, J = 8.2 Hz, 2H), 7.52−7.61 (m, 1H), 7.92−8−02 (m, 1H), 8.09 (d, J = 7.7 Hz, 1H), 8.65 (d, J = 4.7 Hz, 1H); HRMS calcd for $C_{27}H_{37}BrN_4O_6Na$ $(M + Na)^+$: 615.1794. Found: 615.1775.

Pyridine-2-carboxylic Acid {(*S*)-1-[(1*S*,2*S*)-1-(4-Bromobenzyloxymethyl)-2-hydroxy-3-[2-(3-methoxyphenyl)ethylcarbamoyl]propylcarbamoyl}-2-methylpropyl)amide (20). Synthesized according to Procedure A. Purification by column chromatography was performed using chloroform + 1.5% methanol saturated with NH_3 giving **20** in 21% yield. **20**: ^{1}H NMR (CD_3OD, 300 MHz) δ 1.01 (d, J = 6.6 Hz, 3H), 1.04 (d, J = 6.9 Hz, 3H), 2.17−2.28 (m, 1H), 2.31 (app. d, J = 6.9 Hz, 2H), 2.78 (t, J = 7.3 Hz, 2H), 3.41 (t, J = 7.6 Hz, 2H), 3.51−3.67 (m, 2H), 3.77 (s, 3H), 4.09−4.17 (m, 1H), 4.18−4.27 (m, 1H), 4.40−4.50 (m, 3H), 6.71−6.83 (m, 3H), 7.13−7.22 (m, 1H), 7.19 (d, overlapped, 2H), 7.34 (d, J = 8.5 Hz, 2H), 7.54−7.60 (m, 1H), 7.92−8.01 (m, 1H), 8.08 (d, J = 8.0 Hz, 1H), 8.65 (d, J = 4.7 Hz, 1H); HRMS calcd for $C_{32}H_{39}BrN_4O_6Na$ $(M + Na)^+$: 677.1951. Found: 677.1925.

Pyridine-2-carboxylic Acid {(*S*)-1-[(1*S*,2*S*)-1-(4-Bromobenzyloxymethyl)-2-hydroxy-3-(2-phenylaminoethylcarbamoyl)propylcarbamoyl]-2-methylpropyl}amide (21). Synthesized according to Procedure A. Purification by column chromatography was performed using chloroform + 1.5% methanol saturated with NH_3 giving **21** in 19% yield. **21**: ^{1}H NMR (CD_3OD, 300 MHz) δ 1.02 (d, J = 6.9 Hz, 3H), 1.05 (d, J = 6.9 Hz, 3H), 2.19−2.30 (m, 1H), 2.31−2.37 (m, 2H), 3.25 (t, J = 6.0 Hz, 2H), 3.32−3.51 (m, 2H), 3.53−3.68 (m, 2H), 4.11−4.19 (m, 1H), 4.20−4.27 (m, 1H), 4.38−4.49 (m, 3H), 6.60 (t, J = 7.3 Hz, 1H), 6.66 (d, J = 8.1 Hz, 2H), 7.08 (dd, J = 7.3, 8.1 Hz, 2H), 7.18 (d, J = 8.5 Hz, 2H), 7.34 (d, J = 8.5 Hz, 2H), 7.52−7.60 (m, 1H), 7.91−8.00 (m, 1H), 8.09 (d, J = 7.7 Hz, 1H), 8.62−8.69 (m, 1H); HRMS calcd for $C_{31}H_{39}BrN_5O_5$ $(M + H)^+$: 640.2136. Found: 640.2148.

Pyridine-2-carboxylic Acid {(*S*)-1-[(1*S*,2*S*)-1-(4-Bromobenzyloxymethyl)-3-cyclohexylcarbamoyl-2-hydroxypropylcarbamoyl]-2-methylpropyl}amide (22). Synthesized according to Procedure A. Purification by column chromatography was performed using chloroform + 1% methanol saturated with NH_3 giving **22** in 20% yield. **22**: ^{1}H NMR (CD_3OD, 300 MHz) δ 1.02 (d, J = 6.9 Hz, 3H), 1.05 (d, J = 6.9 Hz, 3H), 1.12−1.49 (m, 6H), 1.54−1.95 (m, 4H), 2.19−2.37 (m, 3H), 3.50−3.71 (m, 3H), 4.09−4.17 (m, 1H), 4.18−4.27 (m, 1H), 4.39−4.54 (m, 3H), 7.19 (d, J = 8.5 Hz, 2H), 7.34 (d, J = 8.5 Hz, 2H), 7.52−7.61 (m, 1H), 7.92−8.02 (m, 1H), 8.19 (d, J = 8.0 Hz, 1H), 8.66 (d, J = 4.1 Hz, 1H); HRMS calcd for $C_{29}H_{39}BrN_4O_5Na$ $(M + Na)^+$: 625.2002. Found: 625.2014.

Pyridine-2-carboxylic Acid {(*S*)-1-[(1*S*,2*S*)-1-(4-Bromobenzyloxymethyl)-3-(4-cyanobenzylcarbamoyl)-2-hydroxypropylcarbamoyl]-2-methylpropyl}amide (23). Synthesized according to Procedure A. Purification was performed by HPLC using methanol/H_2O 4:1 + 0.1% TFA yielding **23** in 19%. **23**: ^{1}H NMR (CD_3OD, 300 MHz) δ 1.00 (d, J = 6.6 Hz, 3H), 1.01 (d, J = 6.9 Hz, 3H), 2.11−2.24 (m, 1H), 2.41−2.54 (m, 2H), 3.53−3.69 (m, 2H), 4.14−4.24 (m, 1H), 4.26−4.35 (m, 1H), 4.40 (s, overlapped, 2H), 4.40−4.46 (m, overlapped, 1H), 4.47−4.53 (m, 2H), 7.26 (d, J = 8.5 Hz, 2H), 7.42 (d, J = 8.4 Hz, 2H), 7.47 (d, J = 8.5 Hz, 2H), 7.51−7.62 (m, overlapped, 1H), 7.59 (d, overlapped, J = 8.4 Hz, 2H), 7.89−7.97 (m, 1H), 8.00 (d, J = 8.0 Hz, 1H), 8.65 (d, J = 4.4 Hz, 1H); HRMS calcd for $C_{31}H_{34}BrN_5O_5Na$ $(M + Na)^+$: 658.1641. Found: 658.1642.

Pyridine-2-carboxylic Acid {(*S*)-1-[(1*S*,2*S*)-1-(4-Bromobenzyloxymethyl)-3-butylcarbamoyl-2-hydroxypropylcarbamoyl]-2-methylpropyl}amide (24). Synthesized according to Procedure A. Purification by column chromatography was performed using chloroform + 1.5% methanol saturated with NH_3 giving **24** in 19% yield. **24**: ^{1}H NMR (CD_3OD, 300 MHz): δ 0.92 (t, J = 7.3 Hz, 3H), 1.02 (d, J = 6.6 Hz, 3H), 1.05 (d, J = 6.9 Hz, 3H), 1.29−1.42 (m, 2H), 1.43−1.56 (m, 2H), 2.19−2.30 (m, 1H), 2.33 (app. d, J = 7.4 Hz, 2H), 3.18 (t, J = 7.0 Hz, 2H), 3.51−3.68 (m, 2H), 4.10−4.20 (m, 1H), 4.21−4.29 (m, 1H), 4.38−4.52 (m, 3H), 7.18 (d, J = 8.5 Hz, 2H), 7.33 (d, J = 8.5 Hz, 2H), 7.52−7.59 (m, 1H), 7.93−8.00 (m, 1H), 8.09 (d, J = 7.7 Hz, 1H), 8.65 (d, J = 4.1 Hz, 1H); HRMS calcd for $C_{27}H_{37}BrN_4O_5Na$ $(M + Na)^+$: 599.1845. Found: 599.1851.

Pyridine-2-carboxylic Acid ((*R*)-1-{(1*S*,2*S*)-1-(4-Bromobenzyloxymethyl)-3-[(*S*)-1-((*S*)-1-carbamoyl-3-methylbutylcarbamoyl)ethylcarbamoyl]-2-hydroxypropylcarbamoyl}-2-methylpropyl)amide (25). Synthesized according to Procedure A. Purification by column chromatography was performed using chloroform/ethanol 13:1 + 1.5% methanol saturated with NH_3 giving **25** in 18% yield. **25**: ^{1}H NMR (CD_3OD, 300 MHz): δ 0.83 (d, J = 6.3 Hz, 3H), 0.90 (d, J = 6.0 Hz, 3H), 0.96 (d, J = 6.6 Hz, 3H), 1.01 (d, J = 6.9 Hz, 3H), 1.17 (d, J = 7.1 Hz, 3H), 1.59−1.85 (m, 3H), 2.10−2.29 (m, 1H), 2.47 (dd, J = 5.5, 14.8 Hz, 1H), 2.64 (dd, J = 9.3, 14.8 Hz, 1H), 3.59−3.73 (m, 3H), 4.04 (app. q, J = 7.1 Hz, 1H), 4.18−4.32 (m, 2H), 4.33−4.52 (m, 4H), 7.24 (d, J = 8.5 Hz, 2H), 7.46 (d, J = 8.5 Hz, 2H), 7.54−7.62 (m, 1H), 7.94−8.03 (m, 1H), 8.12 (d, J = 8.0 Hz, 1H), 8.64 (d, J = 4.7 Hz, 1H); HRMS calcd for $C_{32}H_{45}BrN_6O_7Na$ $(M + Na)^+$: 727.2431. Found: 727.2437.

***N*-{(1*S*,2*S*)-1-(4-Bromobenzyloxymethyl)-3-[(*S*)-1-((*S*)-1-carbamoyl-3-methylbutylcarbamoyl)ethylcarbamoyl]-2-hydroxypropyl}-3,4-dichlorobenzamide (26).** Synthesized according to Procedure A. Purification by column chromatography was performed using ethyl acetate/methanol 9:1 + 1% triethylamine providing **26** in 42% yield. **26**: ^{1}H NMR (CD_3OD, 300 MHz): δ 0.89 (d, J = 6.3 Hz, 6H), 1.37 (d, J = 7.4 Hz, 3H), 1.55−1.68 (m, 1H), 1.69−1.86 (m, 2H), 2.48 (dd, overlapped, 1H), 2.53 (dd, overlapped, 1H), 3.75 (app. d, J = 7.4 Hz, 2H), 4.12−4.20 (m, 1H), 4.32−4.44 (m, 3H), 4.47 (d, J = 12.2 Hz, 1H), 4.52 (d, J = 12.2 Hz, 1H), 7.22 (d, J = 8.5 Hz, 2H), 7.42 (d, J = 8.5 Hz, 2H), 7.63 (d, J = 8.4 Hz, 1H), 7.80 (d,

J = 8.4 Hz, 1H), 8.06 (s, 1H); HRMS calcd for $C_{28}H_{35}BrCl_2N_4O_6$-Na $(M + Na)^+$: 695.1015. Found: 695.1025.

***N*-{(1*S*,2*S*)-1-(4-Bromobenzyloxymethyl)-3-[(*S*)-1-((*S*)-1-carbamoyl-3-methylbutylcarbamoyl)ethylcarbamoyl]-2-hydroxypropyl}-2,4,6-trifluorobenzamide (27).** Synthesized according to Procedure A. Purification by column chromatography was performed using ethyl acetate/methanol 9:1 + 1% triethylamine providing **27** in 29% yield. **27**: ^{1}H NMR (CD_3OD, 300 MHz) δ 0.84 (d, J = 6.6 Hz, 3H), 0.85 (d, J = 5.8 Hz, 3H), 1.37 (d, J = 7.4 Hz, 3H), 1.51−1.77 (m, 3H), 2.52 (dd, J = 6.9, 15.1 Hz, 1H), 2.63 (dd, J = 7.4, 15.1 Hz, 1H), 3.64−3.77 (m, 2H), 4.21 (app. q, J = 7.3 Hz, 1H), 4.30−4.46 (m, 3H), 4.49 (d, J = 15.9 Hz, 1H), 4.54 (d, J = 15.9 Hz, 1H), 6.95 (d, J = 7.7 Hz, 1H), 6.98 (d, J = 7.7 Hz, 1H), 7.28 (d, J = 8.5 Hz, 2H), 7.47 (d, J = 8.5 Hz, 2H); HRMS calcd for $C_{28}H_{34}BrF_3N_4O_6$-Na $(M + Na)^+$: 681.1512. Found: 681.1513.

(3*S*,4*S*)-5-(4-Bromobenzyloxy)-4-diphenylacetylamino-3-hydroxypentanoic Acid [(*S*)-1-((*S*)-1-Carbamoyl-3-methylbutylcarbamoyl)ethyl]amide (28). Synthesized according to Procedure A. Purification by column chromatography was performed using ethyl acetate/methanol 9:1 + 1% triethylamine providing **28** in 27% yield. **28**: ^{1}H NMR (CD_3-OD, 300 MHz) δ 0.78 (d, J = 6.1 Hz, 3H), 0.83 (d, J = 6.0 Hz, 3H), 1.29 (d, J = 7.4 Hz, 3H), 1.54−1.71 (m, 3H), 2.38 (app. d, J = 7.4 Hz, 2H), 3.63 (d, J = 6.6 Hz, 2H), 4.20−4.30 (m, 2H), 4.31−4.50 (m, 4H), 5.11 (s, 1H), 7.17 (d, J = 8.5 Hz, 2H), 7.19−7.38 (m, 10H), 7.42 (d, J = 8.5 Hz, 2H); HRMS calcd for $C_{35}H_{43}$-BrN_4O_6Na $(M + Na)^+$: 717.2264. Found: 717.2267.

(3*S*,4*S*)-5-(4-Bromobenzyloxy)-4-(3,3-diphenylpropionylamino)-3-hydroxypentanoic Acid [(*S*)-1-((*S*)-1-Carbamoyl-3-methylbutylcarbamoyl)ethyl]amide (29). Synthesized according to Procedure A. Purification by column chromatography was performed using ethyl acetate/methanol 9:1 + 1% triethylamine providing **29** in 25% yield. **29**: ^{1}H NMR (CD_3OD, 300 MHz) δ 0.90 (d, J = 6.6 Hz, 3H), 0.95 (d, J = 6.3 Hz, 3H), 1.34 (d, J = 7.1 Hz, 3H), 1.55−1.79 (m, 3H), 2.05 (dd, J = 7.4, 14.8 Hz, 1H), 2.14 (dd, J = 7.1, 14.8 Hz, 1H), 2.99 (dd, J = 8.3, 14.2 Hz, 1H), 3.06 (dd, J = 8.0, 14.2 Hz, 1H), 3.32 (dd, overlapped, 1H), 3.42 (dd, J = 6.6, 9.9 Hz, 1H), 3.96−4.05 (m, 1H), 4.10−4.22 (m, 2H), 4.32−4.43 (m, 3H), 4.54 (app. t, J = 8.1 Hz, 1H), 7.09−7.34 (m, 12 H), 7.47 (d, J = 8.5 Hz, 2H); HRMS calcd for $C_{36}H_{45}BrN_4O_6Na$ $(M + Na)^+$: 731.2420. Found: 731.2433.

(3*S*,4*S*)-5-(4-Bromobenzyloxy)-3-hydroxy-4-(2-thiophen-2-ylacetylamino)pentanoic Acid [(*S*)-1-((*S*)-1-Carbamoyl-3-methylbutylcarbamoyl)ethyl]amide (30). Synthesized according to Procedure A. Purification by column chromatography was performed using ethyl acetate/methanol 9:1 + 1% triethylamine providing **30** in 29% yield. **30**: ^{1}H NMR (CD_3OD, 300 MHz) δ 0.83 (d, J = 6.3 Hz, 3H), 0.84 (d, J = 6.3 Hz, 3H), 1.36 (d, J = 7.4 Hz, 3H), 1.53−1.74 (m, 3H), 2.41 (dd, J = 6.9, 14.8 Hz, 1H), 2.48 (dd, J = 7.7, 14.8 Hz, 1H), 3.62 (app. d, J = 6.3 Hz, 2H), 3.75−3.88 (m, 2H), 4.10−4.20 (m, 2H), 4.22−4.30 (m, 1H), 4.31−4.38 (m, 1H), 4.41 (d, J = 12.0 Hz, 1H), 4.47 (d, J = 12.0 Hz, 1H), 6.89−6.97 (m, 2H), 7.19 (d, J = 8.5 Hz, 2H), 7.25 (dd, J = 1.4, 4.9 Hz, 1H), 7.44 (d, J = 8.5 Hz, 2H); HRMS calcd for $C_{27}H_{37}BrN_4O_6SNa$ $(M + Na)^+$: 647.1515. Found: 647.1487.

Benzo[1,3]dioxole-5-carboxylic Acid {(1*S*,2*S*)-1-(4-Bromobenzyloxymethyl)-3-[(*S*)-1-((*S*)-1-carbamoyl-3-methylbutylcarbamoyl)ethylcarbamoyl]-2-hydroxypropyl}-amide (31). Synthesized according to Procedure A. Purification by column chromatography was performed using chloroform/ethanol 13:1 + 1.5% methanol saturated with NH_3 providing **31** in 10% yield. **31**: ^{1}H NMR (CD_3OD, 300 MHz) δ 0.89 (d, J = 6.6 Hz, 3H), 0.90 (d, J = 6.6 Hz, 3H), 1.37 (d, J = 7.2 Hz, 3H), 1.55−1.68 (m, 1H), 1.69−1.83 (m, 2H), 2.47 (dd, J = 6.6, 15.0 Hz, 1H), 2.54 (dd, J = 8.2, 15.0 Hz, 1H), 3.73 (app. d, J = 6.9 Hz, 2H), 4.16 (app. q, J = 7.3 Hz, 1H), 4.33−4.44 (m, 3H), 4.47 (d, J = 12.4 Hz, 1H), 4.52 (d, J = 12.4 Hz, 1H), 6.04 (s, 2H), 6.89 (d, J = 8.3 Hz, 1H), 7.24 (d, J = 8.3 Hz, 2H), 7.38 (d, J = 1.7 Hz, 1H), 7.43 (d, J = 8.2 Hz, 2H), 7.48 (dd, J = 1.7, 8.3 Hz, 1H); HRMS calcd for $C_{29}H_{37}BrN_4O_8Na$ $(M + Na)^+$: 671.1693. Found: 671.1702.

(*S*)-2,3-Dihydro-1*H*-indole-2-carboxylic Acid {(1*S*,2*S*)-1-(4-Bromobenzyloxymethyl)-3-[(*S*)-1-((*S*)-1-carbamoyl-3-methylbutylcarbamoyl)ethylcarbamoyl]-2-hydroxypropyl}amide (32). Synthesized according to Procedure A. Purification by column chromatography was performed using chloroform/ethanol 9:1 + 2% methanol saturated with NH_3 providing **32** in 31% yield. **32**: ^{1}H NMR (CD_3OD, 300 MHz) δ 0.89 (d, J = 6.6 Hz, 3H), 0.92 (d, J = 6.3 Hz, 3H), 1.38 (d, J = 7.1 Hz, 3H), 1.54−1.78 (m, 3H), 2.47 (app. d, J = 7.4 Hz, 2H), 2.97 (dd, J = 8.5, 16.2 Hz, 1H), 3.46 (dd, J = 10.9, 16.2 Hz, 1H), 3.58 (app d, J = 6.6 Hz, 2H), 4.10−4.21 (m, 2H), 4.22−4.32 (m, 1H), 4.33−4.46 (m, 4H), 6.71−6.78 (m, 2H), 7.01−7.08 (m, 2H), 7.10 (d, J = 8.5 Hz, 2H), 7.30 (d, J = 8.5 Hz, 2H); HRMS calcd for $C_{30}H_{40}BrN_5O_6Na$ $(M + Na)^+$: 668.2060. Found: 668.2059.

***N*-{(1*S*,2*S*)-1-(4-Bromobenzyloxymethyl)-2-hydroxy-3-[2-(3-methoxyphenyl)ethylcarbamoyl]propyl}-2,4,6-trifluorobenzamide (33).** Synthesized according to Procedure A. Purification by column chromatography was performed using toluene/ethyl acetate 2:1 providing **33** in 24% yield. **33**: ^{1}H NMR ($CDCl_3$, 300 MHz) δ 2.27 (dd, J = 3.6, 15.1 Hz, 1H), 2.43 (dd, J = 9.6, 15.1 Hz, 1H), 2.78 (t, J = 7.0 Hz, 2H), 3.44−3.57 (m, 2H), 3.69 (app. d, J = 5.5 Hz, 2H), 3.78 (s, 3H), 4.19−4.28 (m, 1H), 4.32−4.39 (m, 1H), 4.50 (app. s, 2H), 5.98−6.06 (b, 1H), 6.49−6.55 (b, 1H), 6.68−6.80 (m, 4H), 7.15−7.24 (m, 2H), 7.19 (d, overlapped, 2H), 7.46 (d, J = 8.3 Hz, 2H); HRMS calcd for $C_{28}H_{28}BrF_3N_2O_5Na$ $(M + Na)^+$: 631.1031. Found: 631.1039.

***N*-[(1*S*,2*S*)-1-(4-Bromobenzyloxymethyl)-3-cyclohexylcarbamoyl-2-hydroxypropyl]-2,4,6-trifluorobenzamide (34).** Synthesized according to Procedure A. Purification by column chromatography was performed using chloroform giving **34** in 27% yield. **34**: ^{1}H NMR ($CDCl_3$, 300 MHz) δ 1.04−1.21 (m, 3H), 1.23−1.43 (m, 2H), 1.54−1.78 (m, 3H), 1.81−1.98 (m, 2H), 2.28 (dd, J = 3.6, 15.1 Hz, 1H), 2.45 (dd, J = 9.6, 15.1 Hz, 1H), 3.65−3.80 (m, 3H), 4.22−4.31 (m, 1H), 4.32−4.41 (m, 1H), 4.50 (app. s, 2H), 5.90−5.99 (b, 1H), 6.49−6.57 (b, 1H), 6.71 (d, J = 8.1 Hz, 1H), 6.74 (d, J = 8.1 Hz, 1H), 7.20 (d, J = 8.4 Hz, 2H), 7.46 (d, J = 8.4 Hz, 2H); HRMS calcd for $C_{25}H_{28}BrF_3N_2O_4Na$ $(M + Na)^+$: 579.1082. Found: 579.1089.

Acknowledgment. We gratefully thank Medivir AB, the Swedish Foundation for Strategic Research (SSF), and Knut and Alice Wallenberg's Foundation for financial support, and Medivir AB for performing the biological testings.

Supporting Information Available: Combustion analyses; HPLC purity measurements. This material is available free of charge via the Internet at http://pubs.acs.org.

References

(1) (a) Murray, M. C.; Perkins, M. E. Chemotherapy of Malaria. *Annu. Rep. Med. Chem.* **1996**, *31*, 141−150. (b) Radding, J. A. Development of Anti-Malarial Inhibitors of Hemoglobinases. *Annu. Rep. Med. Chem.* **1999**, *34*, 159−168. (c) Breman, J. G. The Ears of the Hippopotamus: Manifestations, Determinants, and Estimates of the Malaria Burden. *Am. J. Trop. Med. Hyg.* **2001**, *64*, 1−11. (d) Guerin, P. J.; Olliaro, P.; Nosten, F.; Druilhe, P.; Laxminarayan, R.; Binka, F.; Kilama, W. L.; Ford, N.; White, N. J. *Lancet Infect. Dis.* **2002**, *2*, 564−573. (e) Asojo, O. A.; Gulnik, S. V.; Afonina, E.; Yu, B.; Ellman, J. A.; Haque, T. S.; Silva, A. M. Novel Uncomplexed and Complexed Structures of Plasmepsin II, an Aspartic Protease from *Plasmodium falciparum*. *J. Mol. Biol.* **2003**, *327*, 173−181. (f) Wyatt, D. M.; Berry, C. Activity and inhibition of plasmepsin IV, a new aspartic proteinase from the malaria parasite, *Plasmodium falciparum*. *FEBS Lett.* **2002**, *513*, 159−162.

(2) Francis, S. E.; Sullivan, D. J., Jr.; Goldberg, D. E. Hemoglobin Metabolism in the Malaria Parasite *Plasmodium Falciparum*. *Annu. Rev. Microbiol.* **1997**, *51*, 97−123.

(3) Haque, T. S.; Skillman, A. G.; Lee, C. E.; Habashita, H.; Gluzman, I. Y.; Ewing, T. J. A.; Goldberg, D. E.; Kuntz, I. D.; Ellman, J. A. Potent, Low-Molecular-Weight Non-Peptide Inhibitors of Malarial Aspartyl Protease Plasmepsin II. *J. Med. Chem.* **1999**, *42*, 1428−1440.

(4) (a) Silva, A. M.; Lee, A. Y.; Gulnik, S. V.; Majer, P.; Collins, J.; Bhat, T. N., Collins, P. J.,; Cachau, R. E.; Luker, K. E.; Gluzman, I. Y.; Francis, S. E.; Oksman, A.; Goldberg, D. E.; Erickson, J. W. Structure and Inhibition of Plasmepsin II, a Hemoglobin-Degrading Enzyme from *Plasmodium Falciparum*. *Proc. Natl. Acad. Sci. U.S.A.* **1996**, *93*, 10034−10039. (b) Majer, P.; Collins, J.; Gulnik, S.; Erickson, J.; Pan, W.; Eissenstat, M. A. World Patent WO 97/30072.

(5) (a) Eggelson, K. K.; Duffin, K. L.; Goldberg, D. E. Identification and Characterization of Falcilysin, a Metallopeptidase Involved in Hemoglobin Catabolism within the Malaria Parasite *Plasmodium Falciparum*. *J. Biol. Chem.* **1999**, *274*, 32411−32417. (b) Coombs, G. H.; Goldberg, D. E.; Klemba, M.; Berry, C.; Kay, J.; Mottram, J. C. Aspartic Proteases of *Plasmodium Falciparum* and other Parasitic Protozoa as Drug Targets. *Trends Parasitol.* **2001**, *17*, 532−537.

(6) (a) Banerjee, R.; Francis, S. E.; Goldberg, D. E. Food vacuole plasmepsins are processed at a conserved site by an acidic convertase activity in *Plasmodium falciparum*. *Mol. Biochem. Parsitol.* **2003**, *129*, 157−165. (b) Nezami, A.; Freire, E. The integration of genomic and structural information in the development of high affinity plasmepsin inhibitors. *Int. J. Parasitol.* **2002**, *32*, 1669−1676. (c) Nezami, A.; Kimura, T.; Hidaka, K.; Kiso, A.; Liu, J.; Kiso, Y.; Goldberg, D. E.; Freire, E. High-Affinity Inhibition of a Family of *Plasmodium falciparum* Proteases by a Designed Adaptive Inhibitor. *Biochemistry* **2003**, *42*, 8459−8464.

(7) (a) Francis, S. E.; Gluzman, I. Y.; Oksman, A.; Knickerbocker, A.; Mueller, R.; Bryant, M.; Sherman, D. R.; Rusell, D. G.; Goldberg, D. E. Molecular Characterization and Inhibition of a *Plasmodium Falciparum* Aspartic Hemoglobinase. *Embo. J.* **1994**, *13*, 306−317. (b) Rosenthal, P.; Olson, J. E.; Lee, K.; Palmer, J. T. Antimalarial Effects of Vinyl Sulfone Cysteine Proteinase Inhibitors. *Antimicrob. Agents Chemother.* **1996**, *40*, 1600−1603. (c) Rosenthal, P. J. *Plasmodium Falciparum*: Effects of Proteinase Inhibitors on Globin Hydrolysis by Cultured Malaria Parasites. *Exp. Parasitol.* **1995**, *80*, 272−281. (d) Rosenthal, P. J.; McKerow, J. H.; Rasnick, D.; Leech, J. H. *Plasmodium Falciparum*: Inhibitors of Lysosomal Cysteine Proteinases Inhibit a Trophozite Proteinase and Block Parasite Development. *Mol. Biochem. Parasitol.* **1989**, *35*, 177−184. (e) Rosenthal, P. J.; Wollish, W. S.; Palmer, J. T.; Rasnick, D. Antimalarial Effects of Peptide Inhibitors of a *Plasmodium Falciparum* Cysteine Proteinase. *J. Clin. Invest.* **1991**, *88*, 1467−1472.

(8) Ersmark, K.; Feierberg, I.; Bjelic, S.; Hamelink, E.; Hackett, F.; Blackman, M. J.; Hultén, J.; Samuelsson, B.; Åqvist, J.; Hallberg, A. Potent Inhibitors of the *Plasmodium falciparum* Enzymes Plasmepsin I and II Devoid of Cathepsin D Inhibitory Activity. *J. Med. Chem.* **2004**, *47*, 110−122.

(9) (a) Moon, R. P.; Tyas, L.; Certa, U.; Rupp, K.; Bur, D.; Jacquet, C.; Matile, H.; Loetscher, H.; Grueninger-Leitch, F.; Kay, J.; Dunn, B. M.; Berry, C.; Ridley, R. G. Expression and Characterisation of Plasmepsin I from *Plasmodium falciparum*. *Eur. J. Biochem.* **1997**, *244*, 552−560. (b) Carroll, C. D.; Patel, H.; Johnson, T. O.; Guo, T.; Orlowski, M.; He, Z.-M.; Cavallaro, C. L.; Guo, J.; Oksman, A.; Gluzman, I. Y.; Connelly, J.; Chelsky, D.; Goldberg, D. E.; Dolle, R. E. Identification of Potent Inhibitors of *Plasmodium falciparum* Plasmepsin II from an Encoded Statine Combinatorial Library. *Bioorg. Med. Chem. Lett.* **1998**, *8*, 2315−2320. (c) Carroll, C. D.; Johnson, T. O.; Tao, S.; Lauri, G.; Orlowski, M.; Gluzman, I. Y.; Goldberg, D. E.; Dolle, R. E. Evaluation of a Structure-Based Statine Cyclic Diamino Amide Encoded Combinatorial Library Against Plasmepsin II and Cathepsin D. *Bioorg. Med. Chem. Lett.* **1998**, *8*, 3203−3206. (d) Dolle, R. E.; Guo, J.; O'Brien, L.; Jin, Y.; Piznik, M.; Bowman, K. J.; Li, W.; Egan, W. J.; Cavallaro, C. L.; Roughton, A. L.; Zhao, Q.; Reader, J. C.; Orlowski, M.; Jacob-Samuel, B.; Carroll, C. D. A Statistical-Based Approach to Assessing the Fidelity of Combinatorial Libraries Encoded with Electrophoric Molecular Tags. Development and Application of Tag Decode-Assisted Single Bead LC/MS Analysis. *J. Comb. Chem.* **2000**, *2*, 716−731. (e) Jiang, S.; Prigge, S. T.; Wei, L.; Gao, Y.-E.; Hudson, T. H.; Gerena, L.; Dame, J. B.; Kyle, D. E. New Class of Small Nonpeptidyl Compounds Blocks *Plasmodium falciparum* Development In Vitro by Inhibiting Plasmepsins. *Antimicrob. Agents Chemother.* **2001**, *45*, 2577−2584. (f) Nezami, A.; Luque, I.; Kimura, T.; Kiso, Y.; Freire, E. Identification and Characterization of Allophenylnorstatine-Based Inhibitors of Plasmepsin II, an Antimalarial Target. *Biochemistry* **2002**, *41*, 2273−2280. (g) Asojo, O. A.; Afonina, E.; Gulnik, S. V.; Yu, B.; Erickson, J. W.; Randad, R.; Medjahed, D.; Silva, A. M. Structures of Ser205 Mutant Plasmepsin II from *Plasmodium falciparum* at 1.8 Å in Complex with the Inhibitors rs367 and rs370. *Acta Crystallogr.* **2002**, *D58*, 2001−2008.

(10) (a) Nöteberg, D.; Hamelink, E.; Hulten, J.; Wahlgren, M.; Vrang, L.; Samuelsson, B.; Hallberg, A. Design and Synthesis of Plasmepsin I and Plasmepsin II Inhibitors with Activity in *Plasmodium falciparum*-Infected Cultured Human Erythrocytes. *J. Med. Chem.* **2003**, *46*, 734−746. (b) Nöteberg, D.; Schaal, W.; Hamelink, E.; Vrang, L.; Larhed, M. High-Speed Optimization of Inhibitors of the Malarial Proteases Plasmepsin I and II. *J. Comb. Chem.* **2003**, *5*, 456−464. (c) Dahlgren, A.; Kvarnström, I.; Vrang, L.; Hamelink, E.; Hallberg, A.; Rosenquist, Å.; Samuelsson, B. Solid-Phase Library Synthesis of Reversed-Statine Type Inhibitors of the Malarial Aspartyl Proteases Plasmepsin I and II. *Bioorg. Med. Chem.* **2003**, *11*, 827−841. (d) Dahlgren, A.; Kvarnström, I.; Vrang, L.; Hamelink, E.; Hallberg, A.; Rosenquist, Å.; Samuelsson, B. New Inhibitors of the Malaria Aspartyl Proteases Plasmepsin I and II. *Bioorg. Med. Chem.* **2003**, *11*, 3423−3437. (e) Oscarsson, K.; Oscarson, S.; Vrang, L.; Hamelink, E.; Hallberg, A.; Samuelsson, B. New Potent C_2−Symmetric Malaria Plasmepsin I and II Inhibitors. *Bioorg. Med Chem.* **2003**, *11*, 1235−1246. (f) Ersmark, K.; Feierberg, I.; Bjelic, S.; Hultén, J.; Samuelsson, B.; Åqvist, J.; Hallberg, A. C_2−Symmetric Inhibitors of Plasmodium falciparum Plasmepsin II: Synthesis and Theoretical Predictions. *Bioorg. Med. Chem.* **2003**, *11*, 3723−3733.

(11) Chulay, J. D.; Diggs, C. L. Plasmodium falciparum: assessment of in vitro growth by [^{3}H]hypoxanthine incorporation. *Exp. Parasitol.* **1983**, *55*, 138−146.

(12) See for example: (a) Alterman, M.; Björsne, M.; Mühlman, A.; Classon, B.; Kvarnström, I.; Danielson, H.; Markgren, P.-O., Nillroth, U.; Unge, T.; Hallberg, A.; Samuelsson, B. Design and Synthesis of New Potent C_2−Symmetric HIV-1 Protease Inhibitors. Use of L-Mannaric Acid as a Peptidomimetic Scaffold. *J. Med. Chem.* **1998**, *41*, 3782−3792. (b) Pyring, D.; Lindberg, J.; Rosenquist, Å.; Zuccarello, G.; Kvarnström, I.; Zhang, H.; Vrang, L.; Unge, T.; Classon, B.; Hallberg, A.; Samuelsson, B. Design and Synthesis of Potent C_2−Symmetric Diol-Based HIV-1 Protease Inhibitors: Effects of Fluoro Substitution. *J. Med. Chem.* **2001**, *44*, 3083−3091.

(13) Yanagisawa, H.; Kanazaki, T.; Nishi, T. Synthesis of Statine and Its Analogues. *Chemistry Lett.* **1989**, 687−690.

(14) (a) Arslan, T.; Abraham, A. T.; Hecht, S. M. Structurally Altered Substrates for DNA Topoisomerase I. Effects of Inclusion of a Single 3′-Deoxynucleotide within the Scissile Strand. *Nucleosides Nucleotides* **1998**, *17 (1−3)*, 515−530. (b) Rasmussen, J. R.; Slinger, C. J.; Kordish, R. J.; Newman-Evans, D. D. Synthesis of Deoxy Sugars. Deoxygenation by Treatment with *N,N′*-Thiocarbonyldiimidazole/Tri-n-butylstannane. *J. Org. Chem.* **1981**, *46*, 4843−4846. (c) Rondot, B.; Durand, T.; Girard, J. P.; Rossi, J. C.; Schio, L.; Khanapure, S. P.; Rokach, J. A Free Radical Route to Syn Lactones and other Prostanoid Intermediates in Isoprostaglandin Synthesis. *Tetrahedron Lett.* **1993**, *34*, 8245−8248.

(15) Robinson, P. L.; Barry, C. N.; Bass, S. W.; Jarvis, S. E.; Evans, S. A., Jr. Regioselective Cyclodehydration of Chiral Diols with Diethoxytriphenylphosphorane, Triphenylphosphine-Tetrachloromethane-Potassium Carbonate, and Triphenylphosphine-Diethyl Azodicarboxylate Reagents. A Comparative Study. *J. Org. Chem.* **1983**, *48*, 5396−5398.

(16) Rauter, A. P.; Figueiredo, J.; Ismael, M.; Canda, T.; Font, J.; Figueredo, M. Efficient synthesis of α,β-unsaturated γ-lactones linked to sugars. *Tetrahedron: Asymmetry*, **2001**, *12*, 1131−1146.

(17) Brånalt, J.; Kvarnström, I.; Svensson, S. C. T.; Classon, B.; Samuelsson, B. A New Synthesis of 4-Thiofuranosides via Regioselective Opening of an Episulfide with Allylmagnesium Bromide. *J. Org. Chem.* **1994**, *59*, 4430−4432.

(18) Zuccarello, G.; Abderrahim, B.; Kvarnström, I.; Niklasson, G.; Svensson, S. C. T.; Brisander, M.; Danielsson, H.; Nillroth, U.; Karlén, A.; Hallberg, A.; Classon, B.; Samuelsson, B. HIV-1 Protease Inhibitors Based on Acyclic Carbohydrates. *J. Org. Chem.* **1998**, *63*, 4898−4906.

(19) Müller, M.; Huchel, U.; Geyer, A.; Schmidt, R. R. Efficient Intramolecular Glycosylation Supported by a Rigid Spacer. *J. Org. Chem.* **1999**, *64*, 6190−6201.

(20) Polglase, W. J.; Smith, E. L. Some Peptides and Peptide Derivatives Containing Leucine and Alanine. *J. Am. Chem. Soc.* **1949**, *71*, 3081−3084.

(21) Mehta, A.; Jaouhari, R.; Benson, T. J.; Douglas, K. T. Improved Efficiency and Selectivity in Peptide Synthesis: Use of Triethylsilane as a Carbocation Scavenger in Deprotection of tert-Butyl Esters and *t*-Butoxycarbonyl-Protected Sites. *Tetrahedron Lett.* **1992**, *33*, 5441−5444.

(22) (a) *Novabiochem Catalog and Peptide Synthesis Handbook* 1997/1998, method 16. (b) MilliGen Technical Note 3.10.

(23) Thompson, L. A.; Ellman, J. A. Straightforward and General Method for Coupling Alcohols to Solid Supports. *Tetrahedron Lett.* **1994**, *35*, 9333−9336.

(24) Bartra, M.; Romea, P.; Urpf, F.; Vilarrasa, J. A Fast Procedure for the Reduction of Azides and Nitro Compounds Based on the Reducing Ability of $Sn(SR)_3$−Species. *Tetrahedron* **1990**, *46*, 587−594.
(25) Saftig, P.; Hetman, M.; Schmahl, W.; Weber, K.; Heine, L.; Mossmann, H.; Koster, A.; Hess, B.; Evers, M.; Figura, K. von. Mice deficient for the lysosomal proteinase cathepsin D exhibit progressive atrophy of the intestinal mucosa and profound destruction of lymphoid cells. *EMBO J*. **1995**, *14*, 3599−3608.
(26) Manuscript in preparation.
(27) *Enzymes: A Practical Introduction to Structure, Mechanism, and Data Analysis*, 2nd ed.; Copeland, R. A., Ed.; John Wiley & Sons: New York, 2000.
(28) Cheng, Y.; Prusoff, W. H. Relationship between the Inhibition Constant (K_i) and the Concentration of Inhibitor which Causes 50% Inhibition (IC_{50}) of an Enzymatic Reaction. *Biochem. Pharmacol.* **1973**, *22*, 3099−3108.
(29) Blackman, M. J. *Methods Cell Biol.* **1994**, *45*, 213−220.

JM031106I